FINAL REPORT- AOARD 064092

"Target Tracking and Interception by Aggressive Honeybees"

PI: Mandyam V. Srinivasan

Queensland Brain Institute and School of Information Technology and Electrical Engineering
ARC Centre of Excellence in Vision Science
University of Queensland
St. Lucia, QLD 4072
Australia

Report Documentation Page		Form Approved OMB No. 0704-0188

Public reporting burden for the collection of information is estimated to average 1 hour per response, including the time for reviewing instructions, searching existing data sources, gathering and maintaining the data needed, and completing and reviewing the collection of information. Send comments regarding this burden estimate or any other aspect of this collection of information, including suggestions for reducing this burden, to Washington Headquarters Services, Directorate for Information Operations and Reports, 1215 Jefferson Davis Highway, Suite 1204, Arlington VA 22202-4302. Respondents should be aware that notwithstanding any other provision of law, no person shall be subject to a penalty for failing to comply with a collection of information if it does not display a currently valid OMB control number.

1. REPORT DATE **18 AUG 2010**	2. REPORT TYPE **Final**	3. DATES COVERED **09-02-2007 to 09-01-2010**
4. TITLE AND SUBTITLE **Target Tracking and Interception by Aggressive Honeybees**		5a. CONTRACT NUMBER **FA48690710010**
		5b. GRANT NUMBER
		5c. PROGRAM ELEMENT NUMBER
6. AUTHOR(S) **Mandayam Srinivasan**		5d. PROJECT NUMBER
		5e. TASK NUMBER
		5f. WORK UNIT NUMBER
7. PERFORMING ORGANIZATION NAME(S) AND ADDRESS(ES) **University of Queensland,Brisbane,QLD, Australia,AU,4072**		8. PERFORMING ORGANIZATION REPORT NUMBER **N/A**
9. SPONSORING/MONITORING AGENCY NAME(S) AND ADDRESS(ES) **Asian Office of Aerospace Research & Development, (AOARD), Unit 45002, APO, AP, 96338-5002**		10. SPONSOR/MONITOR'S ACRONYM(S) **AOARD**
		11. SPONSOR/MONITOR'S REPORT NUMBER(S) **AOARD-064092**

12. DISTRIBUTION/AVAILABILITY STATEMENT
Approved for public release; distribution unlimited

13. SUPPLEMENTARY NOTES

14. ABSTRACT
The contractor characterized and modeled the dynamic properties of the sensorimotor system in aggressive honeybees that mediate the detection, tracking and interception of moving targets.

15. SUBJECT TERMS
Biomimetics, Guidance

16. SECURITY CLASSIFICATION OF:			17. LIMITATION OF ABSTRACT	18. NUMBER OF PAGES	19a. NAME OF RESPONSIBLE PERSON
a. REPORT **unclassified**	b. ABSTRACT **unclassified**	c. THIS PAGE **unclassified**	**Same as Report (SAR)**	**63**	

Standard Form 298 (Rev. 8-98)
Prescribed by ANSI Std Z39-18

FINAL REPORT- AOARD 064092

"Target Tracking and Interception by Aggressive Honeybees"

SUMMARY OF AIMS

This study has investigated how aggressive bees detect and track their targets, to uncover how natural visual systems have evolved to perform the highly exquisite and demanding task of detecting a moving object in the environment, and then tracking it and intercepting it quickly and unerringly.

SUMMARY OF RESEARCH CONDUCTED

We have

(i) Designed and constructed an experimental chamber for studying and filming the behavior of aggressive bees (Fig. 1).

Figure 1. External view of experimental chamber, showing projector and computer for display of targets on a screen inside the chamber.

ii) Designed and developed a number of methods for initiation of aggression in honeybee colonies. An example of one of the methods is shown in Fig. 2 and is described later below.
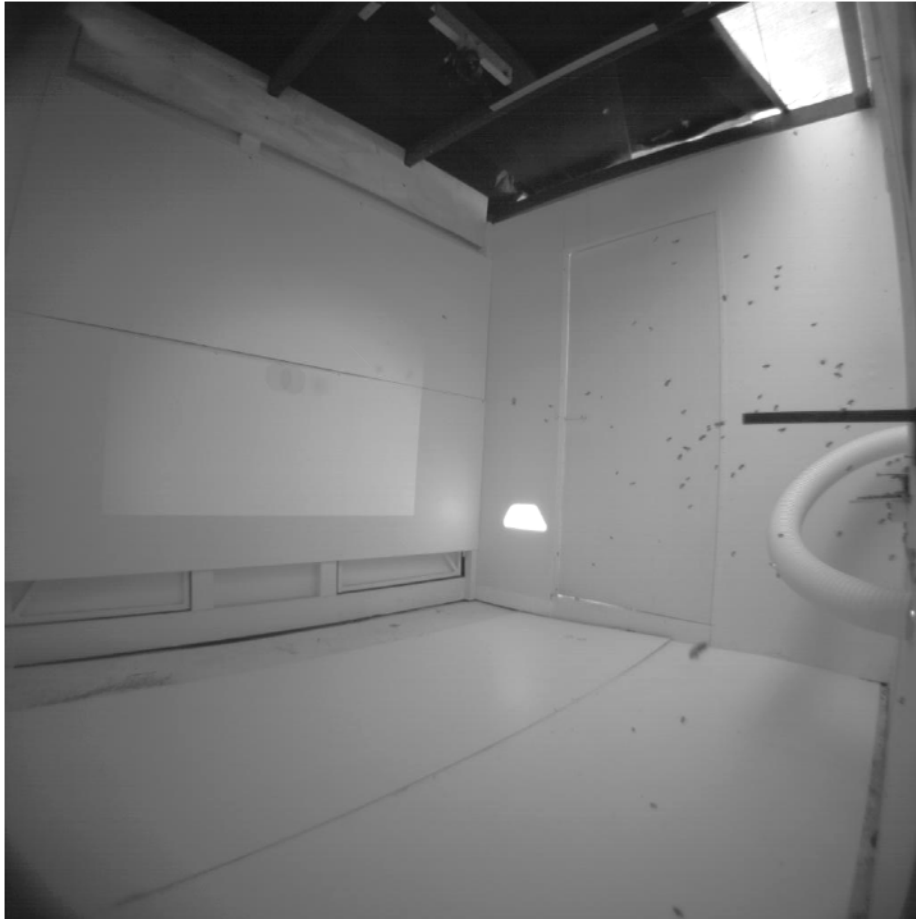

Figure 2. View of specially designed "Aggravator" to create aggression in a honeybee colony

Figure 3. View of aggressive bees attacking a beekeeper's glove

(iii) Set up and calibrated a high-speed stereo camera system for recording the flight trajectories of aggressive bees.

Figure 4. View of inside of experimental chamber, as captured by one of the high-speed stereo cameras positioned at one corner of the chamber. The second stereo camera (not visible) is in the ceiling. The hive entrance is to the right.

(iv) Developed computer algorithms for digitizing, tracking and reconstructing the body positions and orientations of individual aggressive bees pursuing targets in 3 dimensions (see Fig. 21 below).

(v) Compared aggression towards stationary 3-dimensional and 2-dimensional targets.

(vi) Investigated the distribution of aggression towards multiple stationary targets.

 (vii) Designed and tested mechanically-based as well as video-display-based equipment for producing moving targets;

(viii) Set up a computer-controlled visual display to investigate how aggression depends upon the spectral (colour) properties of the target

(ix) Acquired substantial quantitative data on 3-D trajectories of aggressive bees pursuing moving targets

(x) Developed a preliminary mathematical model to characterize the dynamics of target pursuit behavior in aggressive honeybees

(xi) Investigated a novel 'streamlining' response displayed by tethered, flying bees, which is likely to be relevant to achieving high flight speeds and accelerations during aggressive pursuit.

KEY FINDINGS

The key research findings are summarized below:

1. METHODS OF INDUCING AGGRESSION

Two methods were found to be the most effective in eliciting aggression in bee colonies:

(a) ***Alarm pheromone method*** Alarm pheromone was obtained by removing the sting and poison sack from the abdomens of a few bees and placing them on a piece of filter paper, which absorbed the extruded pheromone. The filter paper was then placed in front of the hive entrance. After about a minute, aggressive bees emerged from the hive in considerable numbers. A movie illustrating this procedure is included in the accompanying Powerpoint presentation.

(b) ***Mechanical aggravator method*** A specially designed device consisting of an array of paint brushes mounted on a sliding rod was moved back and forth across the hive entrance (Fig. 2). The moving brushes flicked bees emerging at the entrance, inducing aggression in them. A movie illustrating this procedure is included in the accompanying Powerpoint presentation.

Depending upon the particular colony, method (a) or method (b) was found to be more effective.

2. EXPERIMENTS TO INVESTIGATE TARGET PREFERENCE

(a) 3-D versus 2-D targets

We found that bees in a state of aggression will track and intercept three-dimensional targets, as well as two-dimensional targets projected on a screen. In the case of stationary targets, aggressive bees prefer to attack a three-dimensional target (a hemisphere), as opposed to a two-dimensional target (a flat disc) of equal surface area.

When aggressive bees are offered a choice between a hemispherical sphere and a flat disc (of equal diameter or equal surface area), the bees display a greater frequency of attacks toward the 3-D target when it has the same diameter as the 2-D target, but a lower frequency of attacks when it has the same surface area. This was established by video-filming strikes to the targets using a video camera, over controlled periods of time following initiation of aggression.

These findings demonstrate that bees are capable of visually distinguishing between three-dimensional and two-dimensional objects, and prefer to direct their aggression at the three-dimensional object when it subtends the same visual angle as the two-dimensional object.

The data are summarized in the figures below.
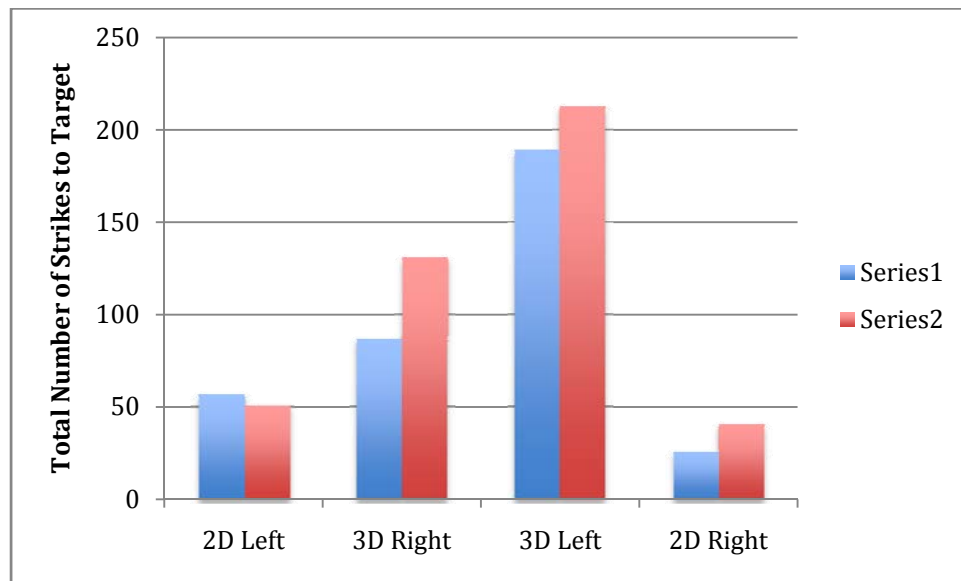
Figure 5. Total number of strikes to a 2-D target and a 3-D target placed side by side. The experiment was conducted twice (Series 1 and Series 2) and repeated each time by swapping the left-right positions of the two targets, to average out any side biases. The data represents the pooled results of experiments with 3-D and 2-D targets that were equal in (a) diameter or (b) surface area.
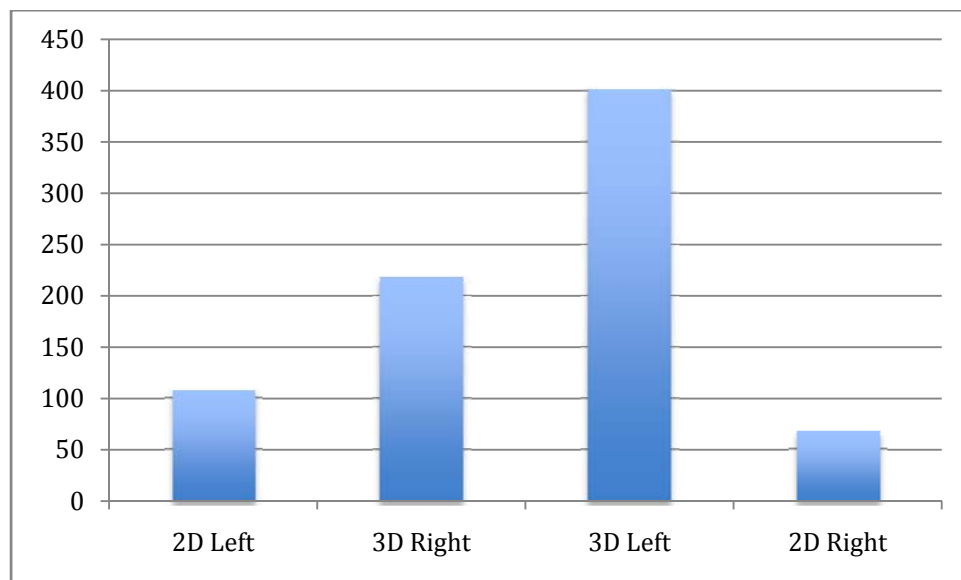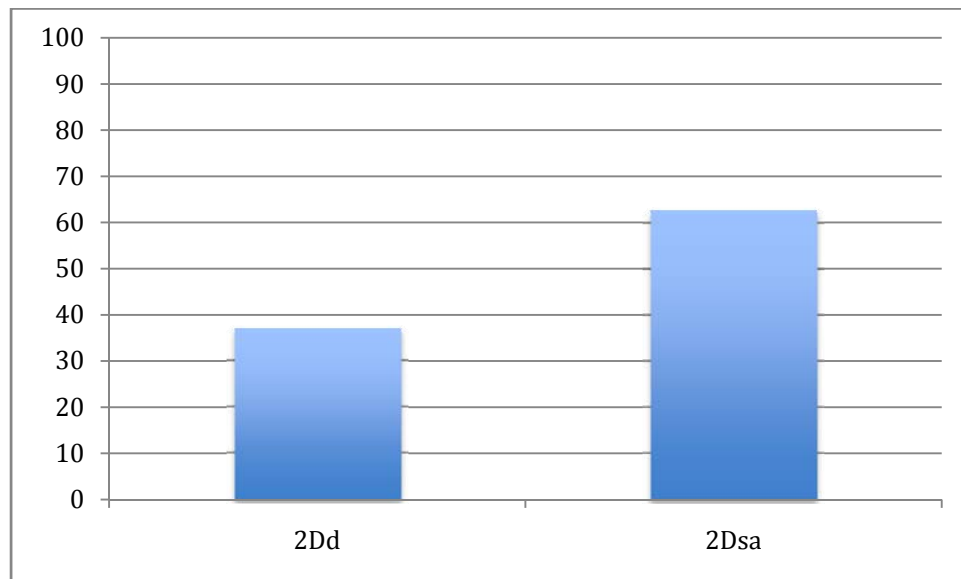

Figure 6. Total number of strikes to each target in the left and right positions. The data are pooled across replicates.
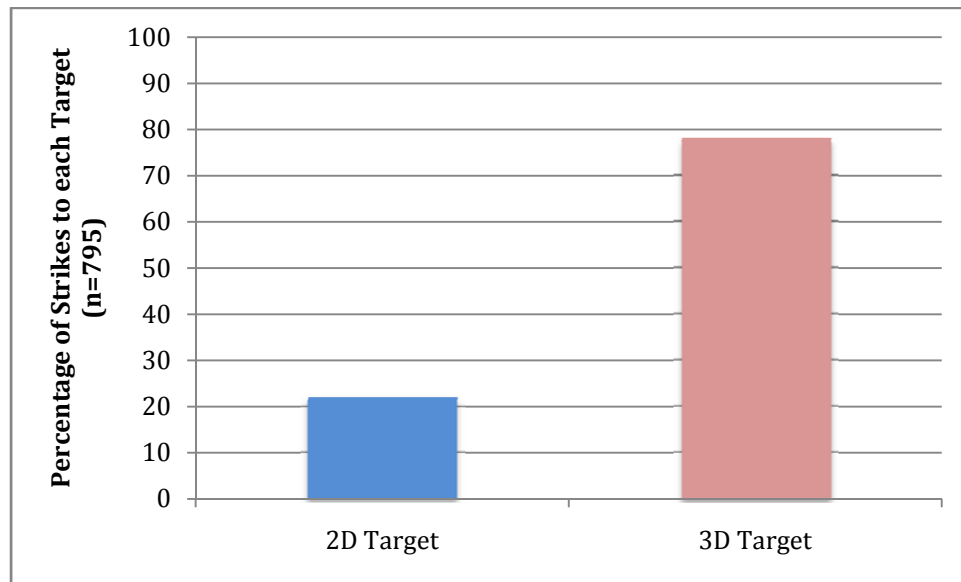
Figure 7. Percentages of strikes to the 2-D and 3-D targets, pooled across replicates and sides.

Figure 8. Percentages of strikes to 2-D targets that are of the same diameter (2Dd) or the same surface area (2Dsa) as the 3-D target. Data are pooled across replicates and sides.

(b) Distribution of strikes over a stationary 2-D target

We video-filmed and analyzed the spatial distribution of strikes over a stationary 2-D target diameter 19 cm. For analysis, the target was subdivided into o (a) 8 equal 45-deg sectors, and (b) an inner circle and an outer annulus of equal area, as shown in Fig. 9.
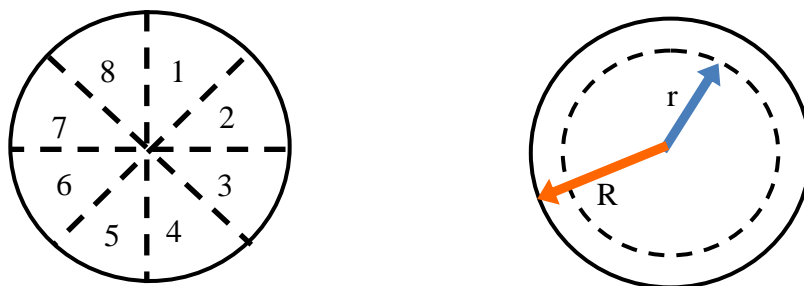

Figure 9. Illustration of subdivision of target into (a) 8 equal 45-deg sectors, and (b) an inner circle and an outer annulus of equal area. In (b) the radius of the inner circle (r) is 70.7% of the radius of the target (R), which ensures that the inner circle and the annulus are of the same area.

The number of strikes to each of these regions was evaluated. The results show that aggressive bees prefer to strike (a) the upper half of the target, rather than the lower half and (b) the boundary of the target, rather than the interior. The strike rate is highest during the first 20 seconds of aggression, after which it decays approximately exponentially as a function of time. The results are summarized in Figs. 10-13 below.
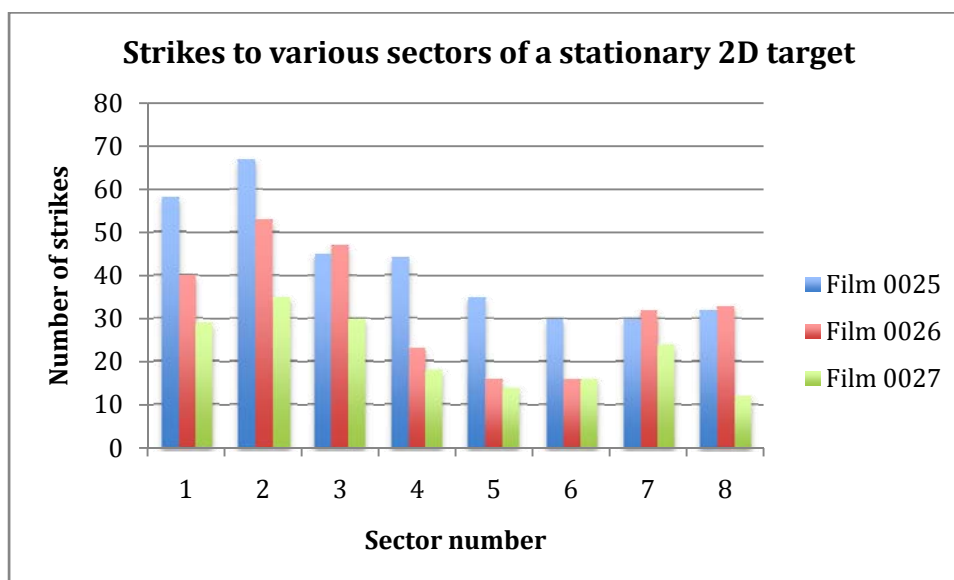
Figure 10. Strikes to each of 8 sectors of a stationary, circular 2-D target of diameter 19 cm. For this analysis, the target is subdivided into eight equal 45-degree sectors, as illustrated in Fig. 9.
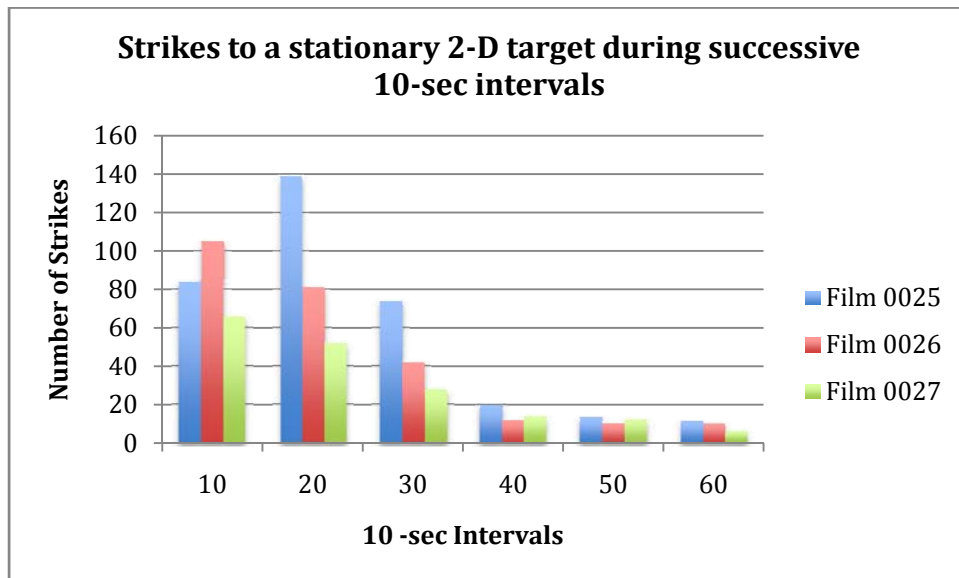
Figure 11. Strikes to the target during successive 10-second intervals, pooled over all sectors.
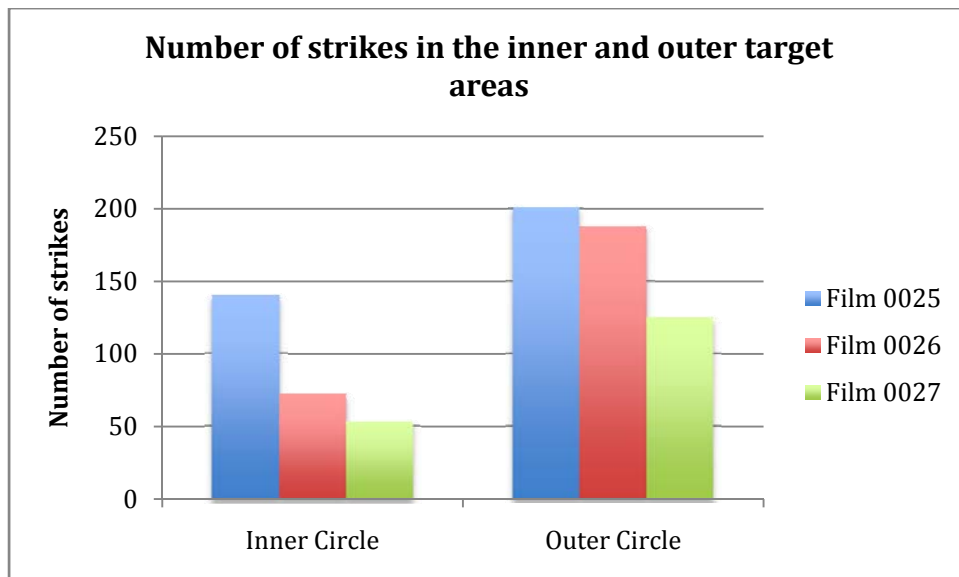
Figure 12. Comparison of strikes to the inner circle and the annulus of the 2-D target (these areas are equal)
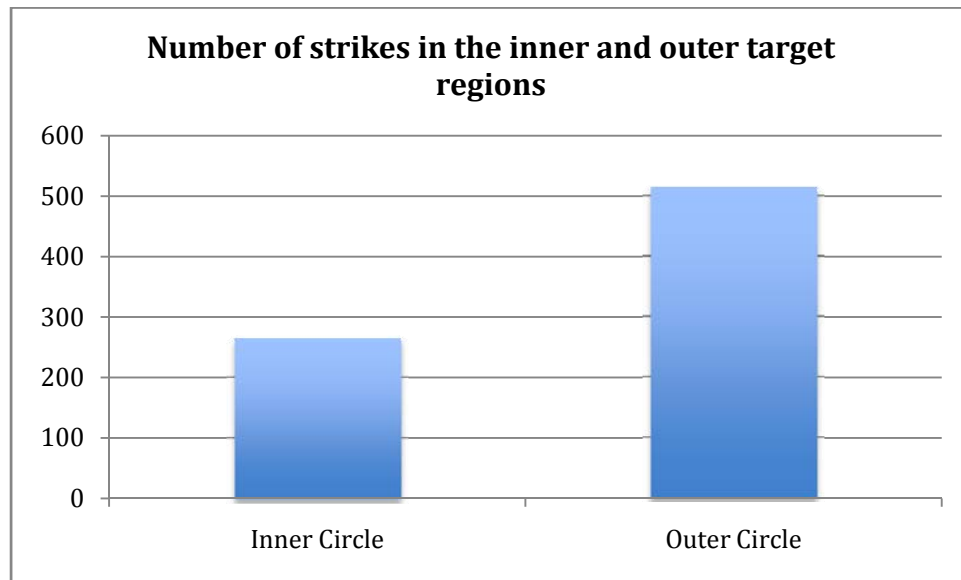
Figure 13. Total numbers of strikes to the inner circle and outer annulus of a circular target, both regions having the same area. Data is pooled over 3 replicates.

(d) Attacks to multiple targets

To examine how bees direct their aggression towards multiple targets, we presented them with a constellation of 9 dark, circular 2-D targets, arranged in a 3x3 array as shown in Fig. 14. Strikes to the targets were recorded by using a video camera to film the display for controlled periods of time following initiation of aggression.
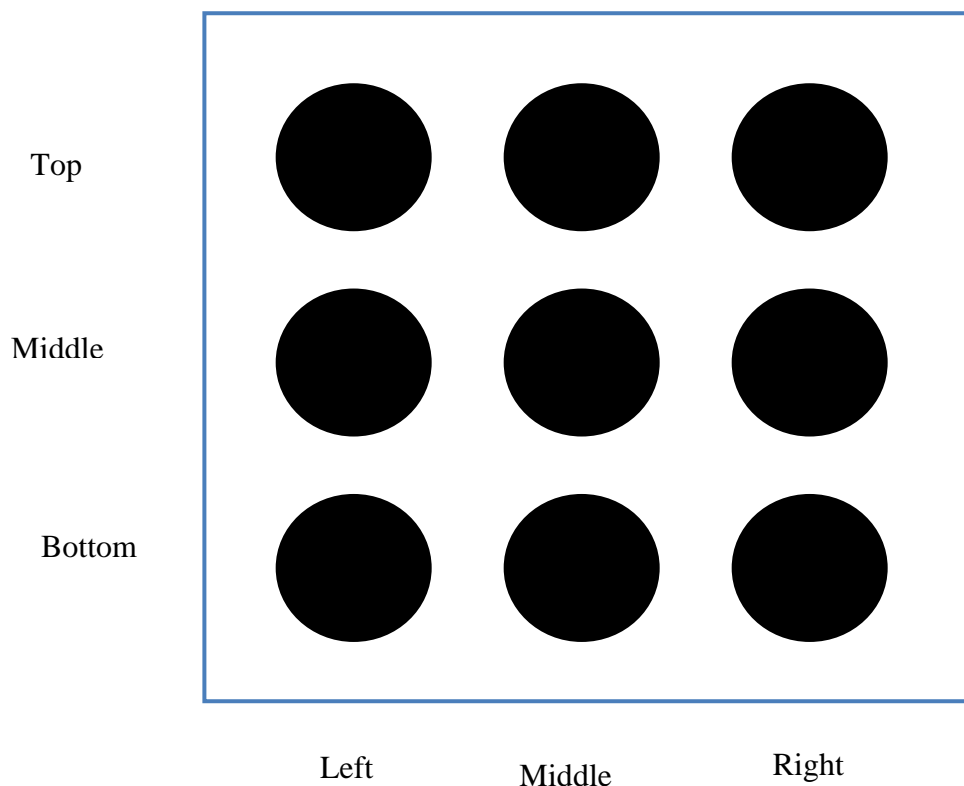
Figure 14. Illustration of target array used to investigate aggression toward multiple targets. The targets were each 9.4 cm in diameter, and were separated by 13 cm (centre to centre).

The results (Fig. 15) show that aggressive bees prefer to strike the peripherally located targets rather than centrally located ones. The central target elicits the lowest strike rate. Furthermore, within each row or column of targets, (or across the two diagonal rows), the middle target is always the one that elicits the lowest strike rate. *This may reflect a strategy to maximize the number of successful strikes, if one assumes that the peripheral targets can hinder, prevent or endanger attacks to the centrally-located targets.*
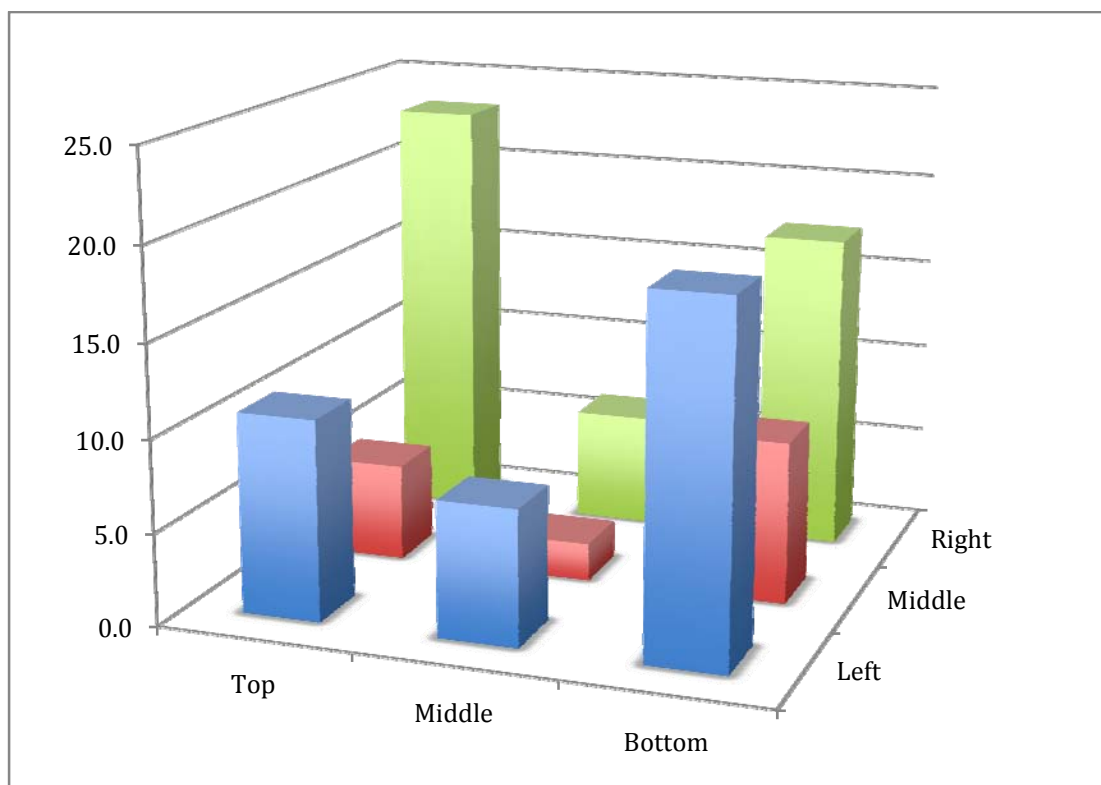

Figure 15. Percentage of strikes (totalling 100%) to each of the nine targets illustrated in Fig. 14.

(c) Spectral properties of target attractiveness

We find that, in general, aggressive bees prefer to strike a dark target on a light background. We have commenced investigating the spectral properties of target attractiveness by comparing the strikes elicited by white, light grey, dark grey and black targets when they are presented against a green background or a blue background, as illustrated in Fig. 16. All of the targets were stationary. The positions of the four targets were randomly interchanged from trial to trial, to average out any positional biases with regard to target selection. Strikes to the targets were recorded by using a video camera to film the display for controlled periods of time following initiation of aggression.
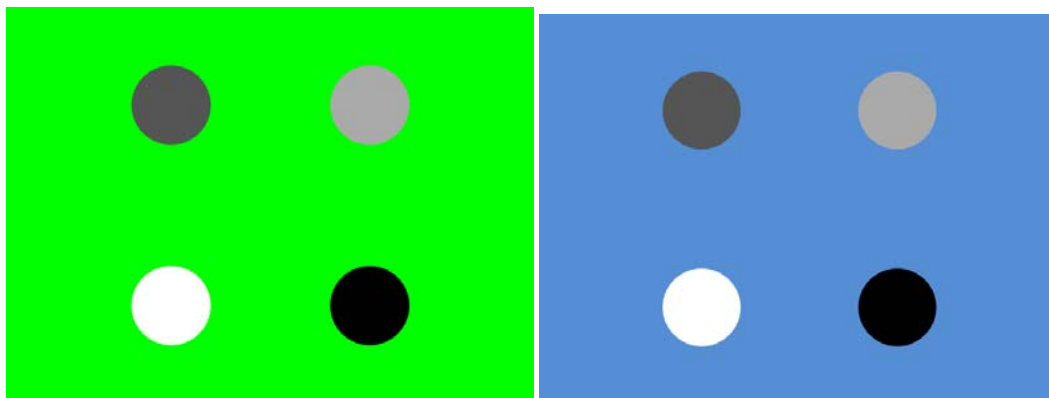
Figure 16. Stimuli for investigating spectral properties of target attractiveness.

The results are shown in Fig. 17. In general, the attractiveness of the target increases as it becomes darker. This is true for both backgrounds, except for the one case of the black target against the green background. *A black target against a blue background attracts the largest percentage of strikes. Thus, aerial targets, which usually appear dark when viewed against a blue sky, are likely to be attacked strongly, as are terrestrial targets when they are approached from below and viewed against the sky.*
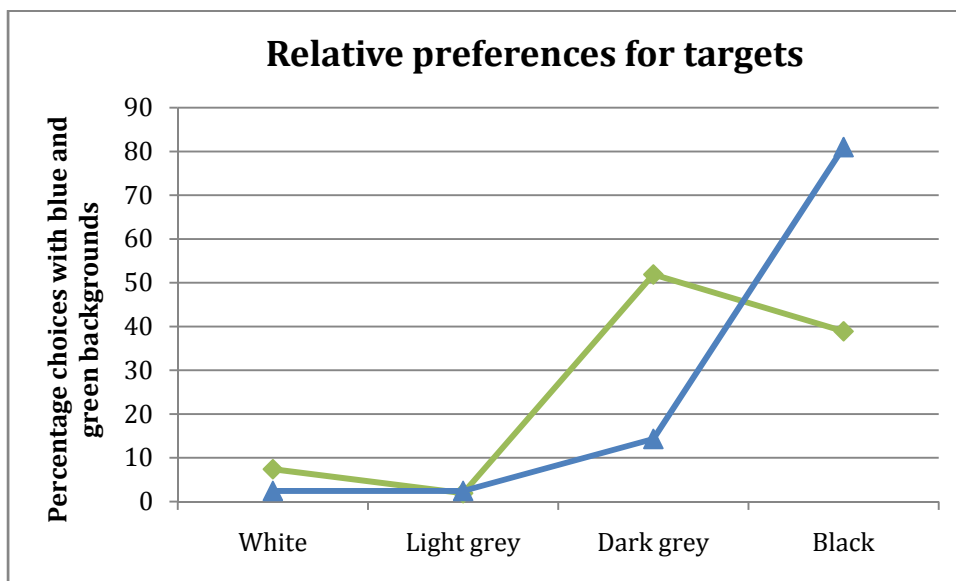
Figure 17. Relative preferences for white, light grey, dark grey and black targets presented against a green background (green curve) or a blue background (blue curve).

(d) Preference for stationary versus moving targets

Aggressive bees were exposed to a visual display projected onto the inside wall of the chamber that faced the hive entrance. The display presented two dark targets of the same diameter. One of the targets was stationary, while the other oscillated from side to side at a uniform velocity (target position versus time was a triangular waveform). Both targets were two-dimensional. Strikes to the targets were recorded by using a video camera to film the display for controlled periods of time following initiation of aggression.

Figure 18. View of video camera for filming and recording strikes to targets and background through a porthole at the rear of the chamber.

The results showed that, during the first minute of aggression, bees do not discriminate between a stationary and a moving target. However, they show a clear preference for the moving target during the second and third minutes. *Thus, bees are able to distinguish between stationary and moving targets, whilst they themselves are in motion.* The data are summarized in Figs. 19 and 20 below.
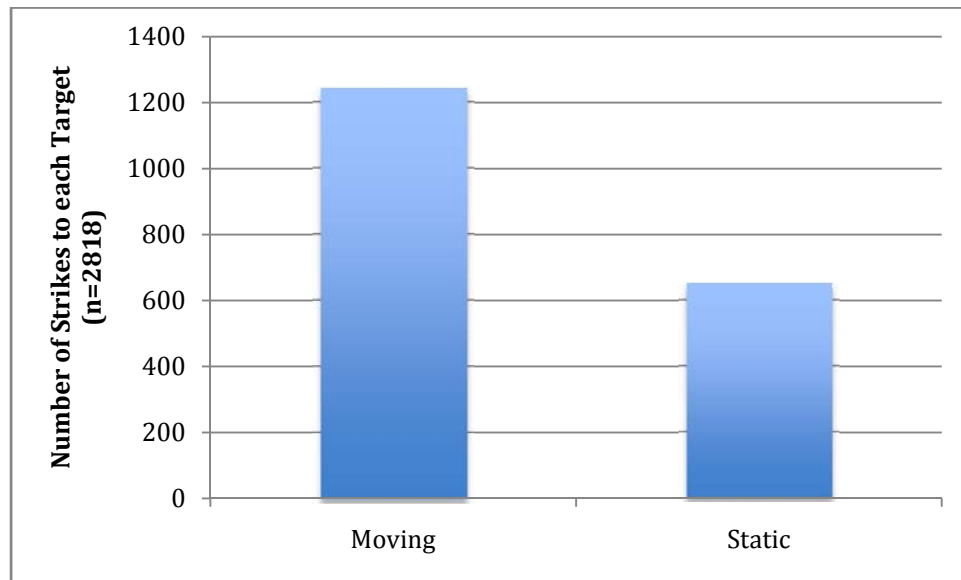
Figure 19. Comparison of numbers of strikes to a stationary versus a moving 2-D target.
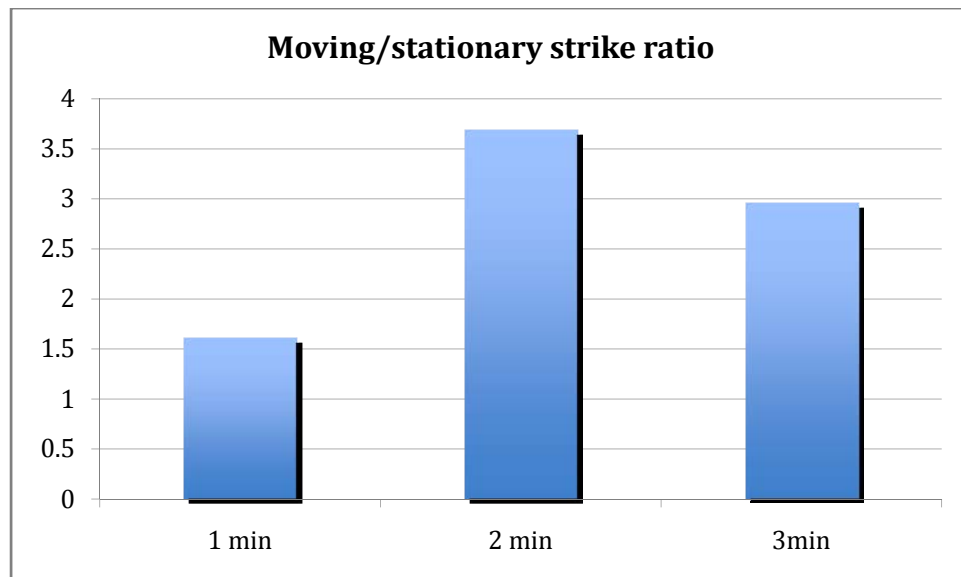
Figure 20. Ratio of strikes elicited by a moving versus a stationary target, measured separately over three 1-minute intervals after onset of aggression.

(2) TRACKING AND INTERCEPTION OF MOVING TARGETS

We have filmed a large number of flights of aggressive bees attacking 3-D targets that (a) oscillate along a straight line in the horizontal plane (b) oscillate along a straight line in the vertical plane and (c) move along a circular trajectory in the vertical plane.

An example of a pursuit trajectory, digitized and reconstructed in 3-D, is shown in Fig. 21. An animation of this reconstruction is included in the accompanying Powerpoint presentation.
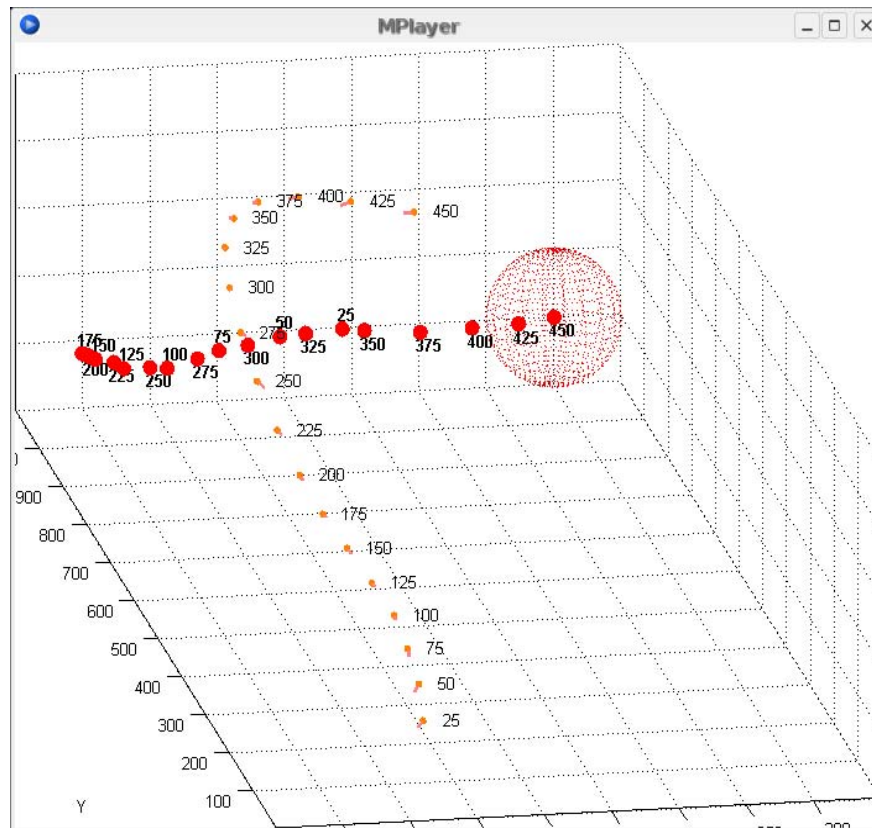
Figure 21. An example showing the reconstruction of the 3-D trajectories of the target (red) and a pursuing aggressive bee (orange). The red dots denoted successive positions of the centre of the sphere, and orange dots and lines denote successive positions and body orientations of the bee. The sphere denotes the current position of the target.

Preliminary analysis of the pursuit trajectories of aggressive bees has revealed that:

(a) Pursuit speed increases approximately linearly as a function of time, i.e. the acceleration is approximately constant. Two examples are shown in Figs. 22 and 23. *These data suggest that aggressive pursuit is achieved by the production of a constant, high thrust and that the acceleration during pursuit is limited primarily by the inertia of the bee, and not by aerodynamic resistance.*
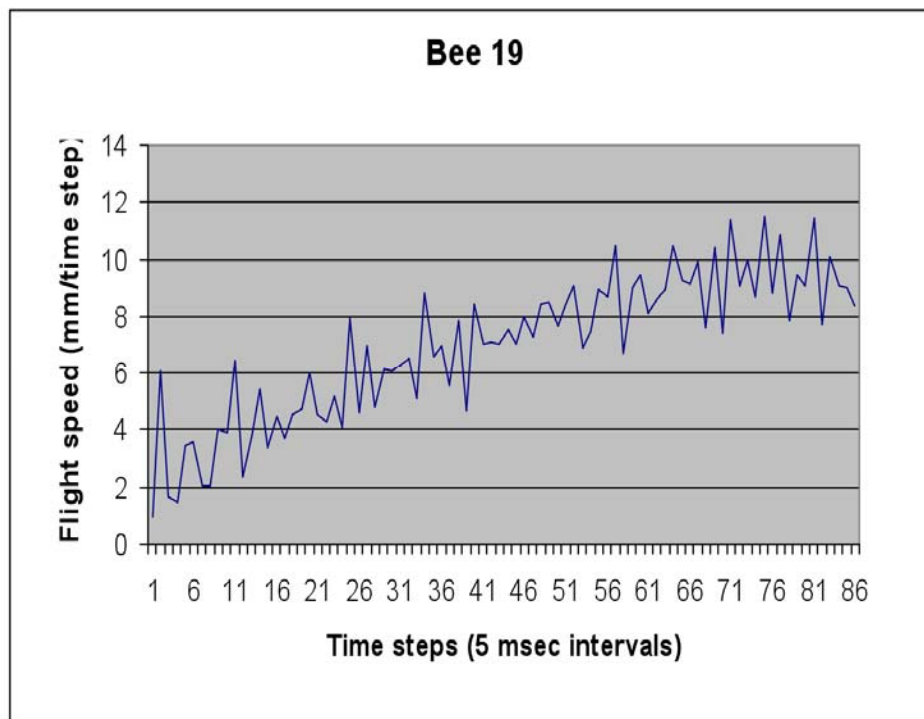
Figure   22. Flight speed versus time for an aggressive bee tracking a moving target (example 1).
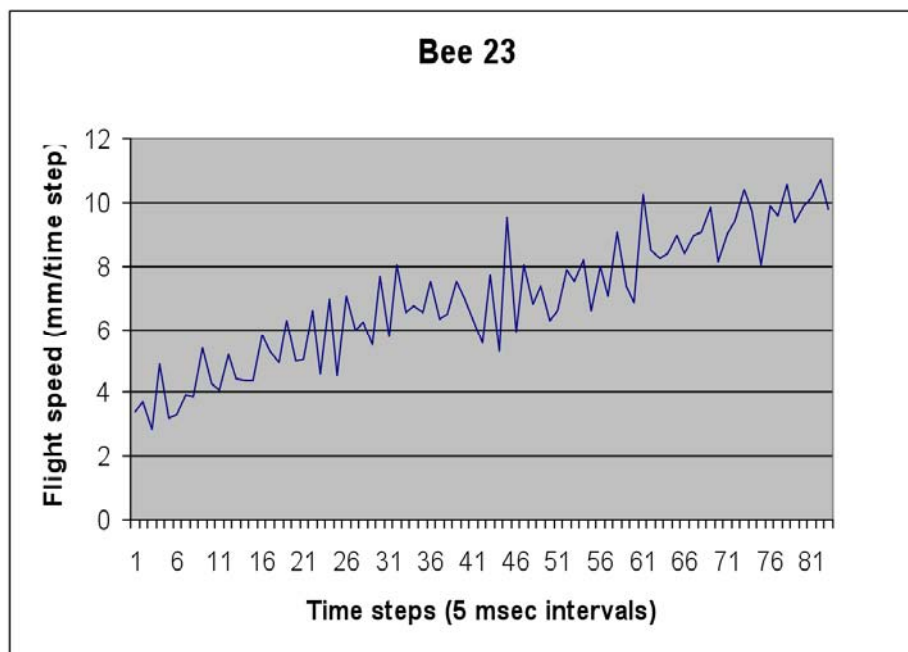
Figure 23. Flight speed versus time for an aggressive bee tracking a moving target (example 2).

The acceleration continues until the time of impact with the target. The target is impacted

at a high velocity (about 2m/sec) and there is little or no deceleration prior to impact. A movie showing the impact is included in the accompanying Powerpoint presentation.

This is in stark contrast to the landing behavior of a non-aggressive foraging bee, which decelerates smoothly as it approaches its target (a food-reward-bearing object). Here, the distance to the target (and therefore the flight speed) decreases exponentially as a function of time, suggesting that, in this case, the landing bee adjusts its flight speed so as to hold constant the rate of expansion of the target (Fig. 24). Additionally, foraging honeybees display a hover phase just prior to touchdown, in which they hover at a distance of about 15 mm from the target. This hover phase, which is illustrated in a movie in the accompanying Powerpoint presentation, never occurs in the case of an aggressive bee.
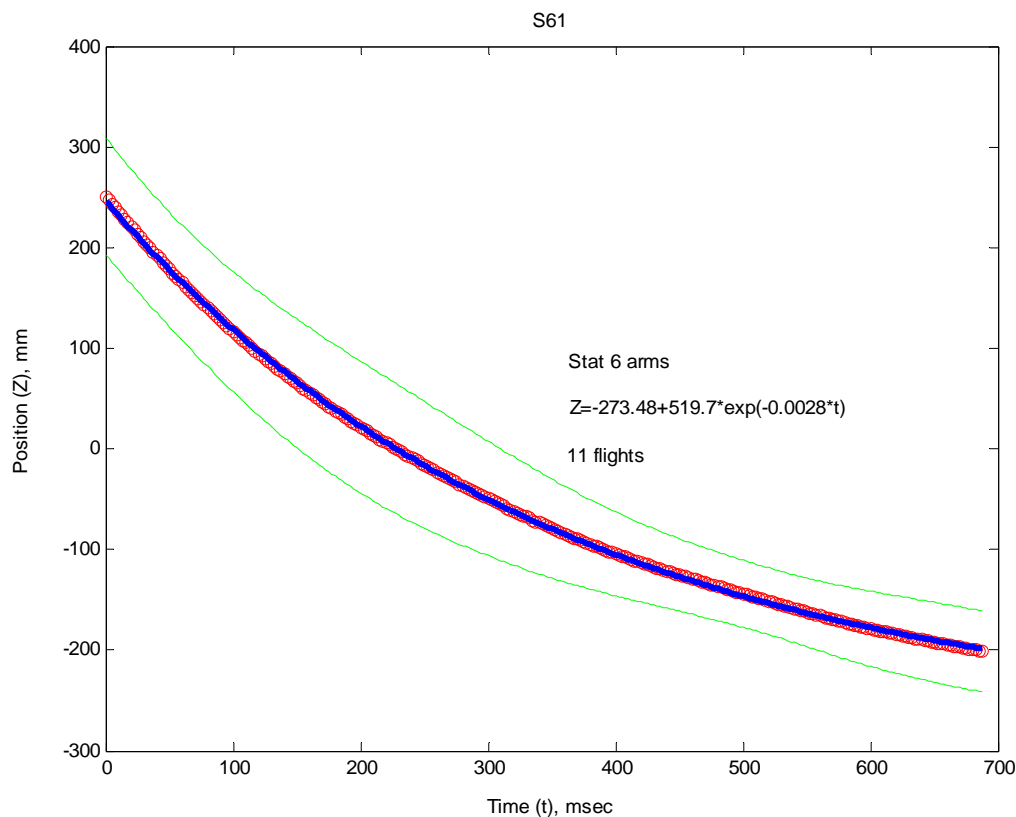
Figure 24. Distance versus time for a foraging (non-aggressive) honeybee approaching a target containing a food reward. The red circles denote mean distance as a function of time, the green curves denote ± standard deviation, and the blue curve represents a fit to an exponential function.

   (b) the turning rate of the bee (yaw rate) is controlled by the angular position of the target, as well as the rate of change of the angular position. This is illustrated in Figs. 25 and 26.
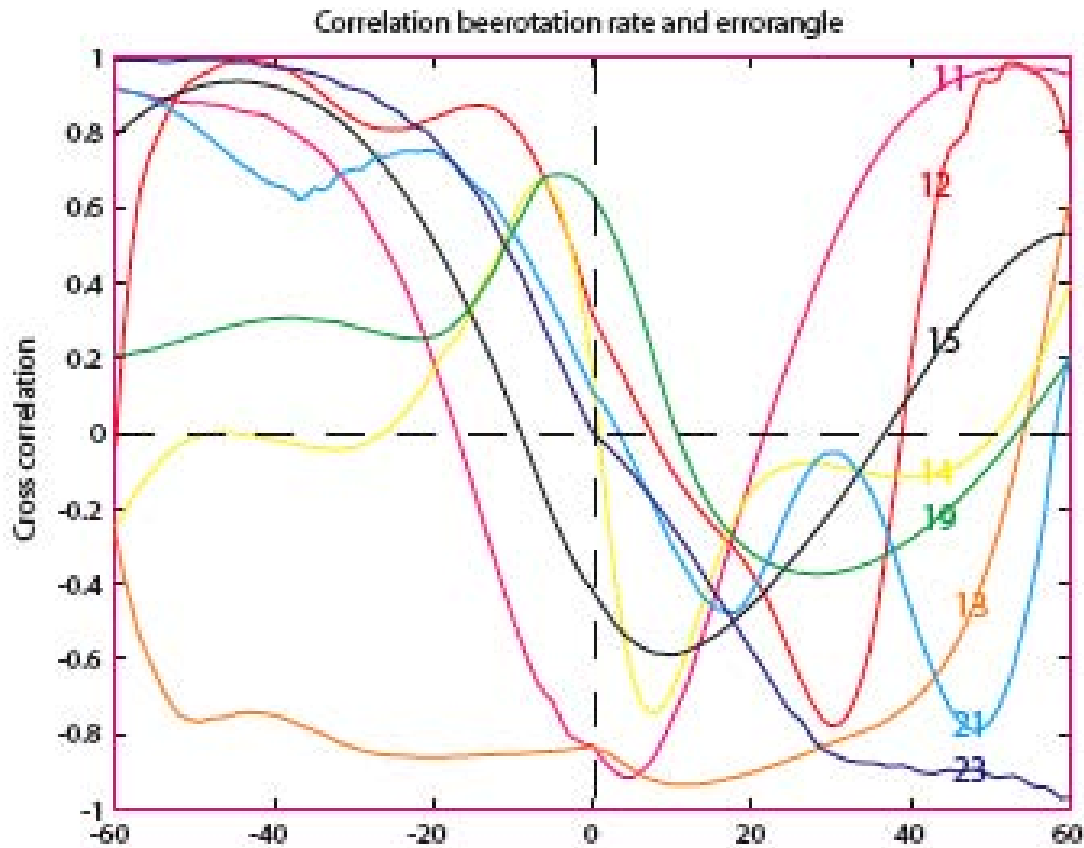
Figure 25. Cross correlation between bee rotation rate (yaw rate) and angular position of target as a function of delay time (in msec, abscissa) for various individual bees.

The cross correlation between the bee rotation rate and the angular position of the target is a maximum when the target angular position is delayed by 30 ms relative to the bee rotation rate. This suggests that the instantaneous yaw rate of the bee is approximately proportional to the angular bearing of the target 30 ms earlier in time. The precise value of this latency varies from bee to bee.
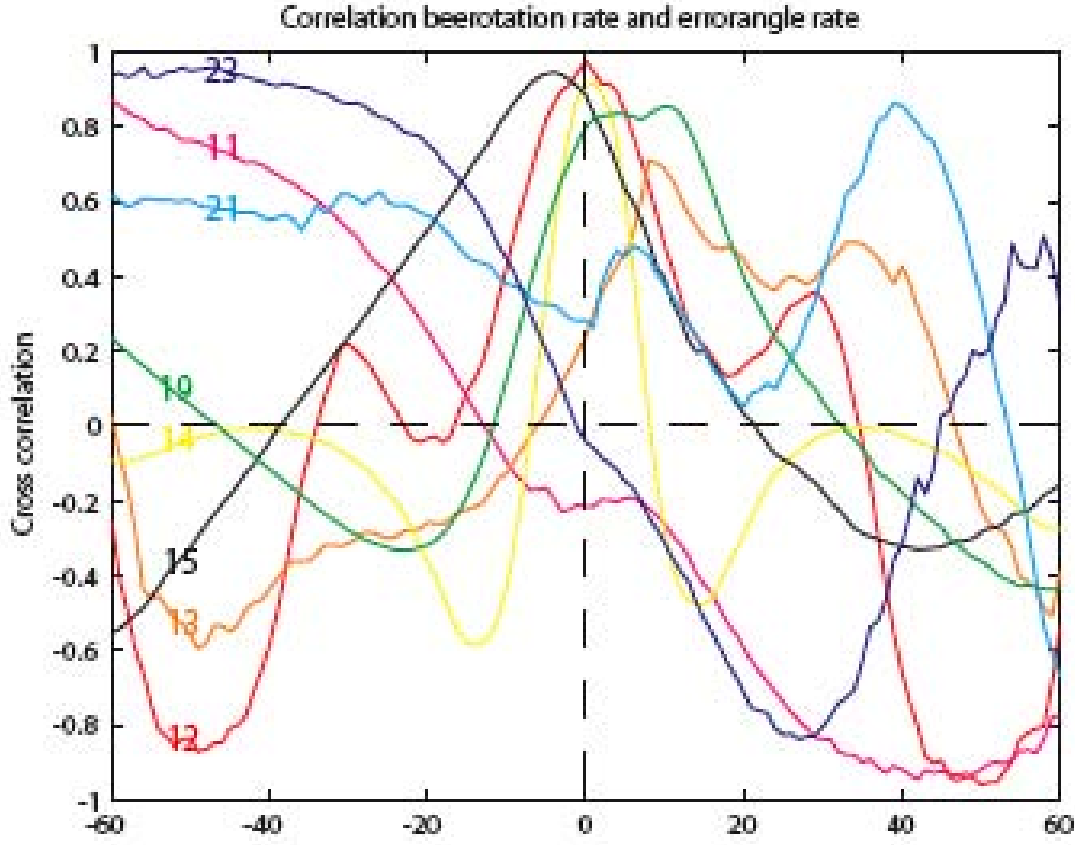
Figure 26. Cross correlation between bee rotation rate (yaw rate) and rate of change of angular position of target as a function of delay (in msec, abscissa) for various individual bees.

The cross correlation between the bee rotation rate and the rate of change angular position of the target is a maximum when the rate of change of angular position is delayed by approximately 0 ms relative to the bee rotation rate. This suggests that the instantaneous yaw rate of the bee is approximately proportional to the current rate of change of the angular bearing of the target.

On the basis of the above data, we have formulated a preliminary model to characterize the dynamics of pursuit behavior of aggressive bees tracking a moving target. The yaw rate ω of the pursuing bee is given by

$$\omega = \alpha\theta(t - T) + \beta\acute{\theta}(t) \tag{1}$$

where θ is the angular bearing of the target in the bee's eye, and $\acute{\theta}$ is the rate of change of this angular bearing (see Fig. 27). T is the time delay associated with the response to the target bearing, α is a gain parameter that relates the yaw rate to the angular bearing of the target, and β is a gain parameter that relates the yaw rate to the rate of change of the angular bearing of the target.
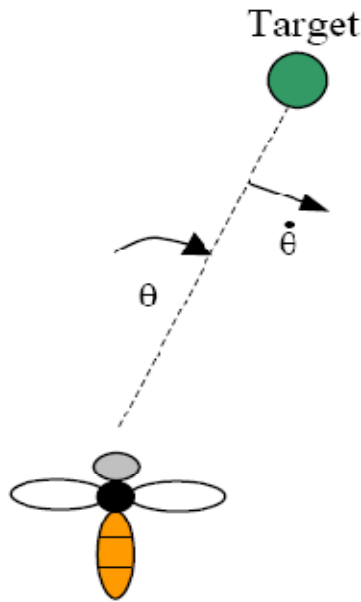
Figure 27. Illustration of dynamical model for characterizing pursuit behavior. θ is the angular bearing of the target in the bee's eye, and $\dot{\theta}$ is the rate of change of this angular bearing.

We have carried out preliminary simulations of this model, which we have implemented in Matlab. One example of the results is shown in Fig. 28, which compares the observed trajectory of a bee (black symbols) pursuing a target, with the trajectory predicted by the model (red symbols), using the following parameters:

(a) Constant acceleration of 4000mm/sec^2
(b) α=20.0
(c) β=0.7
(d) T =0.03 sec

It is evident that the model captures the essential elements of the dynamics of the pursuit behaviour. An animation of the simulation is included in the accompanying Powerpoint presentation.

Further work is required to fine-tune the mode and to evaluate its applicability to the large number of pursuit events that we have recorded.
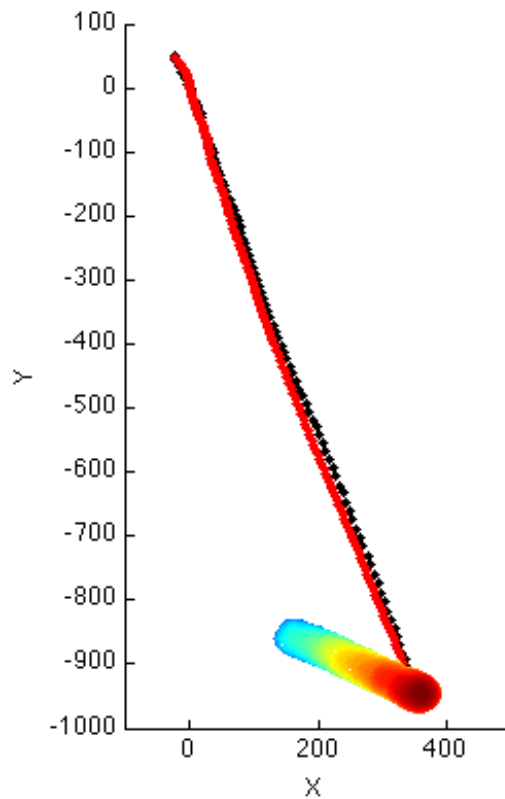
Figure 28. Illustration of one example of the results from a model simulating the dynamics of pursuit behavior. The circles show successive positions of the target [blue (past) → red (present)]. The black symbols denote the reconstructed trajectory of an aggressive bee pursuing the target, and the red symbols denote the trajectory predicted by the model.

3. INVESTIGATION OF A 'STREAMLINING' RESPONSE IN FLYING HONEYBEES

During the course of this research we have become interested in examining how honeybees achieve the high flight speeds and accelerations that we have observed when they are in the aggressive state. We have recently discovered a novel 'streamlining' response, exhibited by tethered, flying honeybees, in which the abdomen is held in a raised position when the visual system is exposed to a pattern of image motion (i.e. a flow field) that is characteristic of forward flight. We believe that this visually evoked response, which can be elicited without exposing the insect to any airflow, serves to reduce the aerodynamic drag that would otherwise be produced by the abdomen during real flight. The streamlining response is critically dependent on the presence of appropriate image motion in the frontal as well as the rear fields of view. It is relatively insensitive to variations of stimulus contrast, exhibiting values close to the maximum

for contrasts in the range of 0.3 – 1.0, and is therefore capable of operating robustly in a wide variety of natural environments. These findings also underscore the importance of using panoramic stimulation for the study of visually guided flight in insects.

The experimental procedures and key results are summarized below, and a movie illustrating the 'streamlining' response is included in the accompanying Powerpoint presentation.
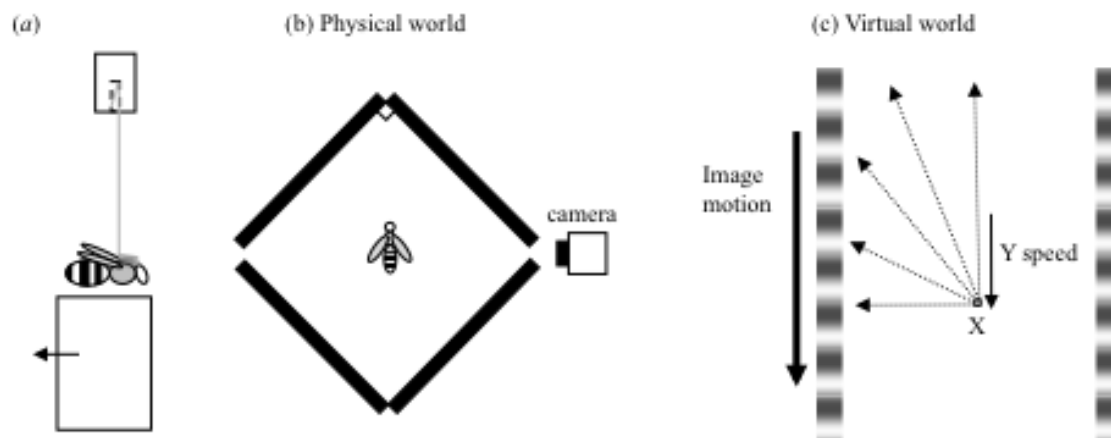
Figure 29

The abdominal posture of tethered honeybees was examined as they flew in a virtual reality setup. The bees were tethered to the horizontal end of an L-shaped metallic rod. Flight was initiated by lowering a supporting platform. (B) Each honeybee was placed in the centre of an arena composed of four monitors. A video camera was used to film a side view of the bee in flight. (C) The virtual scene consisted of an infinite tunnel composed of two walls lined with vertically oriented red and white sinusoidal gratings. The honeybee was at a virtual distance of X units from each of the tunnel walls, and experienced virtual forward motion at a speed of Y units per display frame.
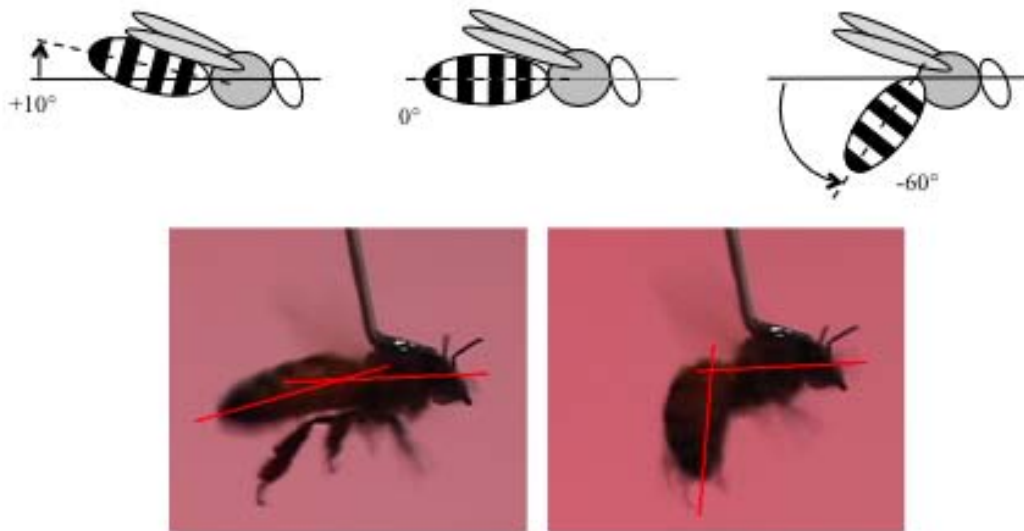
Figure 30

Illustration of the measurement of the streamlining response, defined as the orientation of the abdomen relative to the thorax. The upper row of sketches illustrates the definition of the response, and the lower row shows two examples of how this is used to measure the response.
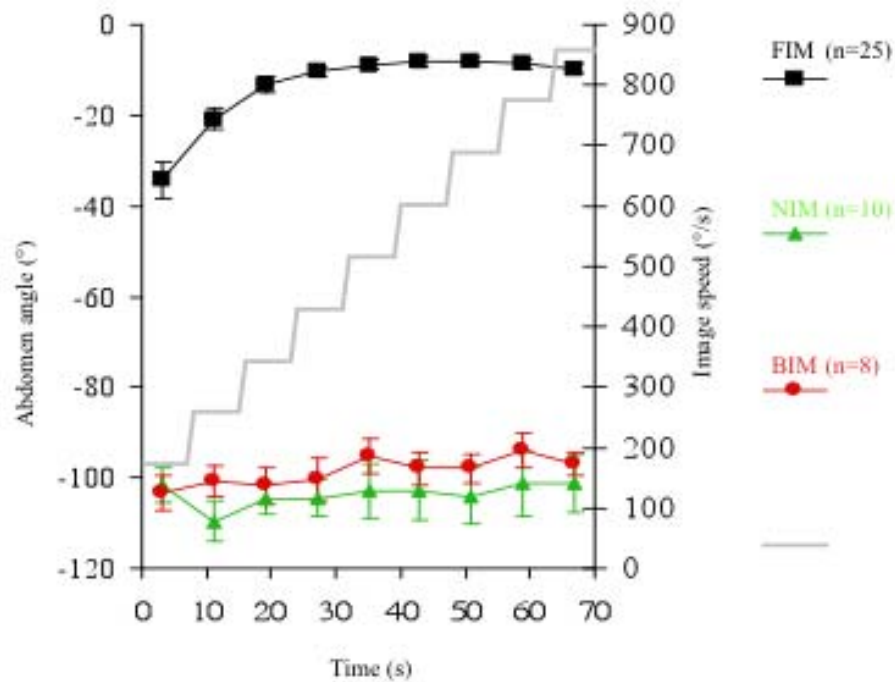
Figure 31

Comparison of streamlining responses induced by forward image motion (FIM), no image motion (NIM) and backward image motion (BIM). The grey staircase displays the progressively ascending stimulus speed (see Methods). Each data point shows mean abdomen angle ± standard error of the mean. Note the comparatively small variability in the responses when bees were experiencing forward image motion.
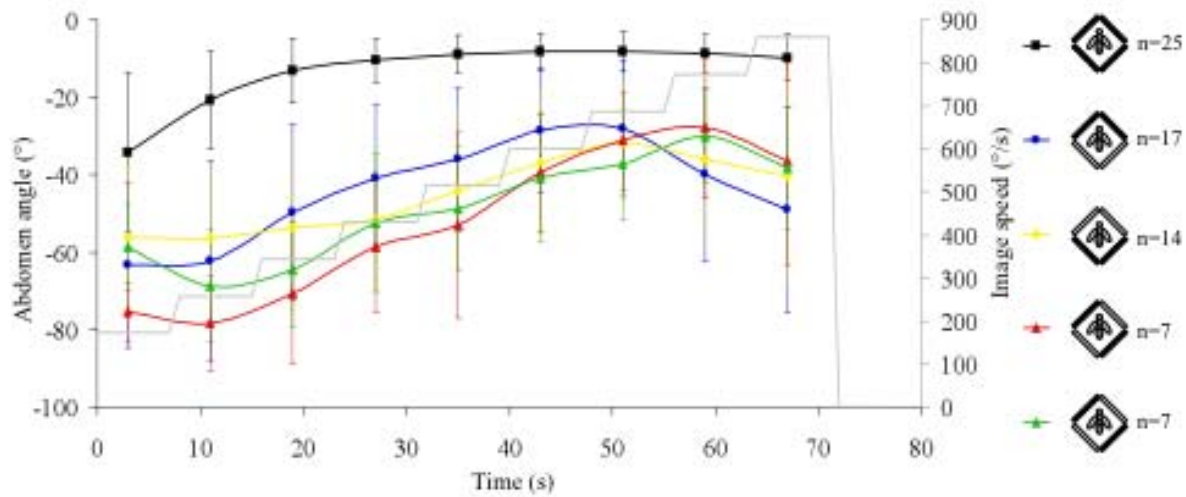
Figure 32

Streamlining responses of tethered bees in experiments using various configurations of two monitors (coloured symbols), compared with the four-monitor configuration (black symbols). All flights were presented with the ascending image motion speed protocol, as indicated by the grey staircase. Each data point shows mean abdomen angle ± standard deviation. Only data from bees that repeatedly exhibited continuous flight were analysed.
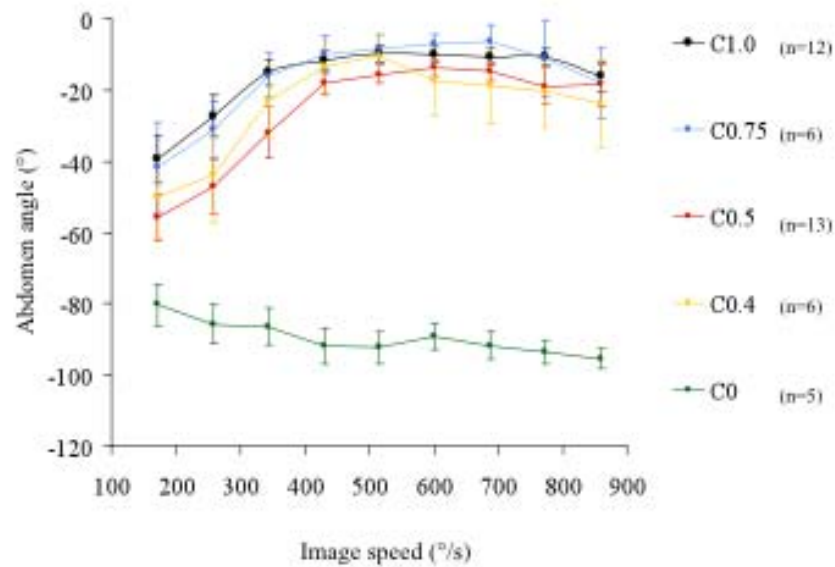
Figure 33

Effect of stimulus contrast on the streamlining response. Variation of abdomen orientation with stimulus speed for five different contrasts, as shown in the index. Each data point shows the mean abdomen angle ± standard error of the mean.

A manuscript describing this study is in preparation (copy attached).

Mandyam V. Srinivasan

Queensland Brain Institute and School of Information Technology and Electrical Engineering
ARC Centre of Excellence in Vision Science
University of Queensland

1   Title Page

2

3   **Honeybee flight: A novel 'streamlining' response**

4

5   Tien Luu[1], Allen Cheung[1], David Ball[1] and Mandyam V. Srinivasan[1,2]

6

7   Author affiliations:

8

9

10   [1] *The University of Queensland, Queensland Brain Institute and School of Information*

11   *Technology and Electrical Engineering, Brisbane, Queensland 4072, Australia*

12

13   [2] *ARC Centre of Excellence in Vision Science*

14

15

16

17

18

20

21

22

23

24

25

26

27

28

29

30

31

32

33

34

35   **Summary**

36

37   Animals that move rapidly through the air can save considerable energy by reducing the drag

38   that they need to overcome during flight. We describe a novel 'streamlining' response in

39   tethered, flying honeybees in which the abdomen is held in a raised position when the visual

40   system is exposed to a pattern of image motion that is characteristic of forward flight. This

41   visually evoked response, which can be elicited without exposing the insect to any airflow,

42   presumably serves to reduce the aerodynamic drag that would otherwise be produced by the

43   abdomen during real flight. The response is critically dependent on the presence of

44   appropriate image motion in the frontal as well as the rear fields of view. Thus, our results

45   also underscore the importance of using panoramic stimulation for the study of visually

46   guided flight in insects.

47
48
49
50

Introduction

It is abundantly clear that all creatures that move rapidly -- in the air, on the ground or under water – would save considerable locomotive energy if their bodies were shaped, or adjusted, to minimize the drag that is produced by the medium through which they move. For example, sharks, tuna and mackerel possess fusiform shapes that enable high swimming speeds to be achieved with relatively low drag (Schmidt-Nielsen, 1984; Bailey, 1997).

While it is of interest to examine whether the bodies of certain animals have evolved to reduce drag, it is also pertinent to ask whether animals can actively change, or adapt, the shapes of their bodies to cope with the increased drag that inevitably accompanies higher speeds of locomotion. This would seem to be important, because the force due to drag theoretically increases as the square of the speed at which the body moves through the medium (Batchelor, 2000). In principle, an animal could achieve 'active' streamlining of this kind by sensing its motion through the medium either mechanically through the use, of, say, mechanosensory hairs or organs to sense airspeed during flight (Goodman, 2003), or through vision, by sensing the motion of the image of the environment in the eye.

Do animals achieve active streamlining? Here we ask whether honeybees use vision-based cues to streamline their bodies at high flight speeds. We find that bees indeed possess a visually-driven 'streamlining' response, whereby an increase in the image velocity experienced by the bee causes the abdomen to be raised higher, thus partially counteracting the increased drag.

As an insect flies through the environment, its eyes experience various patterns of image motion – also known as 'optic flow' patterns - which depend upon how the insect moves in relation to its surroundings. Research over the past fifty years has shown that insect flight is controlled by optic flow in a number of different ways. For example, the well-known 'optomotor' response enables a flying insect to stabilize its attitude with respect to the world by sensing the patterns of optic flow that are generated by its rotations about the yaw, pitch and roll axes (or combinations thereof) and delivering appropriate commands to the flight motor system to counteract these rotations (Götz, 1965; Reichardt, 1969; Srinivasan and Bernard, 1977; Collett et al., 1993; Krapp and Hengstenberg, 1996; Egelhaaf et al., 2004). Fruit flies (David, 1979, 1982; Fry et al., 2009) and honeybees (Srinivasan et al., 1996; Baird et al., 2005) regulate the speed of their flight by holding constant the magnitude of the optic

85   flow that is experienced by the eyes. Collisions with obstacles are avoided by detecting and

86   steering away from regions in the visual field that are associated with unusually large image

87   speeds (Srinivasan et al., 1993; Srinivasan and Zhang, 1997) or rapid expansion of the image

88   (Tammero and Dickinson, 2002). Collision-free flight through narrow passages is achieved

89   by balancing the magnitudes of the optic flow that are experienced by the two eyes

90   (Srinivasan et al., 1991; Srinivasan et al., 1993; Srinivasan et al., 1996). Smooth landings on

91   a horizontal surface are achieved by holding constant the rate of motion of the image of the

92   surface as the surface is approached (Srinivasan et al., 2000).

93

94   Here we examine whether, and, if so, how, optic flow affects body posture during flight, by

95   filming tethered bees flying in a virtual-reality arena that simulates the optic flow that would

96   be generated by forward flight in a tunnel. We find that the simulated forward flight evokes a

97   'streamlining' response in which the bee raises its abdomen, lifting it progressively higher as

98   the speed of the image is increased. This streamlining response is mediated visually, because

99   it is displayed by tethered bees flying in still air, and ceases when the image stops moving.

100   Presumably, the streamlining response serves to reduce the aerodynamic drag that would

101   otherwise be produced by the abdomen during real flight.

102

103

104

105   **Materials and Methods**

106

107   *Bees:* Adult forager honeybees were used in all of the experiments. They were identified as

108   those carrying pollen on their hind legs. The bees were anesthetized in a refrigerator for 20-

109   30 min, after which they were taken out one at a time for tethering.

110

111   *Tethering:* While the bee was anaesthetized, the base of an L-shaped metal rod (see Fig. 1)

112   was attached to the thorax by a small globule of dental glue, which was cured using blue

113   (440-480 nm) light (~40 s). Adhesion to the tether was facilitated by gently shaving the hair

114   on the thorax using a scalpel blade. The bee was then housed in a Styrofoam box in which the

115   temperature was maintained at 26-28°C. A beaker of water, placed inside the box, provided

116   an environment with the appropriate humidity.

117

118   *The experimental arena*: Four 24" LCD monitors (Dell 2408WFP) were arranged on a table

119   to form a square arena. A small (~2 cm) gap was provided at the two lateral corners of the

120   arena to allow a video camera to film the bee in side view (Fig. 1B). The bee was tethered

121   and positioned in the centre of the virtual environment by attaching the upper end of the L-

122   shaped rod to an adjustable metallic arm (not shown). This arm allowed the head of the bee to

123   be positioned in the centre of the arena, at a height midway between the base and top of the

124   monitors. The bee faced one corner of the arena. The table was covered with a 60 cm x 90 cm

125   sheet of black cardboard. All experiments were performed under fluorescent lighting.

126

127   *Virtual reality environment:* Images were created on the four monitors to provide a

128   panoramic virtual environment (Fig. 1). The LCD monitors were driven by a PC (Intel Quad

129   Core CPU Q9300 2.5GHz, 3GB RAM, Windows XP 2002, DirectX 9.0) with two dual head

130   NVIDIA GeForce 8800 GT video cards. The monitors had the following settings: resolution

131   1920x1200 pixels, refresh rate 60Hz. Since the monitors used LCD displays, there was no

132   60Hz flicker.

133

134   A program was written that simulated the visual effects of the movement of an observer

135   within a custom-designed virtual world. The virtual world consisted of an (apparently)

136   infinite tunnel with a blue ceiling, a dark floor, and side walls lined with a sinusoidal grating

137   composed of alternating red and white bars. The red bars would have appeared as (almost)

138   black bars to the bee, because the colour red falls outside the bee's visible spectrum (Menzel

139   and Blakers, 1976; Chittka et al., 1993). Red was used rather than black, to facilitate viewing

140   and filming of the tethered bee against the background of the visual display.

141

142   [Insert Fig. 1 here]

143

144   The program to create the display was written in C++ and used the DirectX API software to

145   create four 'viewports' of the virtual world, each displayed by one monitor, with the virtual

146   camera position geometrically matched to the centre of the arena. Each monitor displayed one

147   quadrant of the virtual world – forward right, forward left, rear left, and rear right. A software

148   interface, written in Python, enabled customization of the virtual world and control of the

149   virtual position and motion of the observer within it. For a bee flying along a virtual tunnel,

150   the maximum image velocity as experienced by the eyes (the maximum optic flow rate, OFR)

151   occurs in the lateral viewing direction, i.e. in a viewing direction at 90° to the direction of

152   flight. For a simulated linear grating speed of Y units/frame, a frame rate of 60/s and a

153   simulated flight along a trajectory that is X units from either wall, this maximum OFR (in °/s)

154   is given by

155

156
$$OFR(°/s) = \left(\frac{60Y}{X}\right)\left(\frac{180}{\pi}\right).$$

157

158   We used a stimulus protocol that simulated flight at a progressively increasing speed, namely,

159   Y = 0.02, 0.03, 0.04, 0.05, 0.06, 0.07, 0.08, 0.09 and 0.1 units/frame. The width of the

160   simulated tunnel (2X) was 0.8 units. The height of the simulated tunnel was 1.0 unit. This

161   staircase of simulated flight speeds generated the following OFRs: 172, 258, 344, 430, 516,

162   602, 688, 773 and 859 °/s respectively. Each epoch of stimulus speed was 8s in duration, thus

163   producing a stimulus that lasted for 72 s in each trial.

164

165   *Calibration of stimulus contrast*

166

167   Sinusoidal gratings of four different contrast levels were used. These contrasts (as defined

168   below) were nominally set to 1.0, 0.75. 0.5 and 0.4, for both the green and blue channels in

169   the 24-bit RGB bitmaps generated using Matlab. The red channel was kept constant at

170   maximum value over the entire bitmap. These grating bitmaps were tessellated to build the

171   long virtual tunnels (described above). However, subsequent measurement and calibration of

172   the various gratings, as described below, revealed that the actual contrasts of these gratings

173   were 0.72, 0.54. 0.36 and 0.29 (or about 72% of the nominal contrast). It is the actual values

174   that are used to report the results.

175

176   The contrasts of the gratings were measured as follows. First, the radiant spectrum of the

177   monitors was measured using an Ocean Optics USB2000+ spectrometer calibrated for

178   wavelength and intensity. Spectra were measured for illumination from a small patch within

179   the centre of the white bar of the sinusoidal grating, as well as within the centre of the red

180   bar. The relative photon flux emitted by each of these patches was obtained by integrating

181   their respective spectra over a spectral window of 300 nm – 600 nm, which represents the

182   visible spectrum of the honeybee (Menzel and Blakers, 1976; Chittka et al., 1993). Denoting

183   the results of this integration for the white and the red bars by I_{max} and I_{min}, respectively, the

184   contrast C of the grating was calculated as $C = (I_{max} - I_{min})/(I_{max} + I_{min})$. This quantity,

185   known as the Michelson contrast, is the commonly used measure of contrast for sinusoidal

186   gratings (Michelson, 1927). It can assume a maximum value of 1.0 when the dark bar emits

187   no light ($I_{min} = 0$), and a minimum value of 0.0 when the dark and bright bars have the same

188   intensity ($I_{max} = I_{min}$).

189

190   In all experiments but one, the Michelson contrast of the grating was set at a high value

191   (C=0.72 in the experiments shown in Figs 3, 4 and 5). In one experiment, which investigated

192   the effect of stimulus contrast, response versus speed curves were obtained for a series of

193   contrasts, as shown in figure 6.

194

195   *Data acquisition and analysis*

196

197   A Samsung video camera (VP-HMX20C, 25 frames per second, 1920x1080 resolution) was

198   used to film the side view of the bee. The video clips were analyzed to measure the

199   orientation of various parts of the body, using a Matlab digitization program written in-house.

200   The program computed the orientation of the line joining any two manually digitized points

201   in the image. It was used to measure the orientation of two lines. One line, connecting the

202   head to the thorax, was defined to be the orientation of the thorax. Another line, connecting

203   the front and rear ends of the abdomen, was defined to be the orientation of its long axis. The

204   program calculated the difference between these two orientations (Fig. 2). This difference,

205   representing the orientation of the abdomen relative to the thorax, was defined as the

206   abdomen angle, or the response. The response was positive or negative, according to whether

207   the abdomen was elevated or depressed relative to the thorax. Responses measured in this

208   way were averaged over the last 4 seconds of each 8-second epoch of stimulus speed, thus

209   giving an average measurement of the honeybee's steady-state response to each of the 9

210   stimulus speeds. Typically, the abdominal response reached a new steady state within 1-3s

211   following each new stimulus speed (data not shown).

212

213   *Statistical analysis*

214

215   All statistical analyses were performed using the software package SPSS/PASW Statistics

216   18.0 (2009). We analyzed the abdominal responses from two independent series of

217   experiments to evaluate the effect of grating contrast and monitor configuration, respectively.

218   In each case, we first performed two-way repeated measures ANOVA to investigate the

219   effect of each independent variable, at all OFRs of the stimulus protocol. If a significant

220   effect was detected, post-hoc pairwise comparisons (*t*-tests, with Bonferroni adjustment for

221   the family-wise Type I error rate) were performed. Note that for the mains effect of interest in

222   each case (monitor configuration or grating contrast), there was no detectable violation of the

223   sphericity assumption.

224

225   *Comparison of responses elicited by two and four monitors*: Abdominal responses were

226   compared across the various two-monitor configurations, and across two- and four-monitor

227   configurations, all at full grating contrast (C=0.72). Only responses from honeybees that

228   experienced all the different configurations were used for this particular comparison (n=7).

229   Since a significant effect was only detected when the 4-monitor data was included, post-hoc

230   tests were only performed in the latter case. These statistical results are shown in Tables A1

231   and A2.

232

233   *Variation of response with stimulus contrast:* Abdominal angles were compared across the

234   various stimulus contrast levels (0.29, 0.36, 0.54 and 0.72), with and without the control

235   condition of zero-contrast (0.00), all using the four-monitor configuration. Only responses

236   from honeybees that experienced all the different contrasts (including 0.00) were used for this

237   particular comparison (n=6). Since a significant effect was only detected when the zero-

238   contrast data was included, post-hoc tests were only performed in that case. These statistical

239   results are shown in Tables A3 and A4.

240

241

242   [Insert Fig. 2 here]

243

244   *Flight initiation*

245   For each flight trial, a tethered honeybee was placed in the centre of the arena and a platform

246   (Fig. 1) was raised from under the bee until all of the bee's tarsae made contact with it, with

247   the legs in their natural resting position. As soon as the visual stimulus was started, the

248   platform was retracted from under the bee. At the end of the visual stimulus, the platform

249   was restored to its pre-flight position so that the bee's legs were again resting on it, thus

250   preventing further flight. The platform was covered with wax paper (which was frequently

251 replaced) to ensure a firm, but smooth support that could not be gripped by the bee's tarsal

252 hooks, thus ensuring trouble-free release of the feet at the onset of flight. After each flight the

253 bee was fed 10 μL of 1 M sucrose solution and returned to the humid box.

254

255 **Results**

256

257 We found that in all bees tested, the action of removing the platform from under the bee's

258 legs immediately triggered wing beat activity. This is the well-known 'tarsal reflex' (Fraenkel

259 1932; Chadwick 1953). At this instant, the abdomen would also drop and assume a hanging

260 orientation. Bees would then occasionally fly for a few seconds. However, combining the

261 platform removal with the onset of a moving visual stimulus enhanced the duration of flight

262 considerably, typically at least two minutes, as we shall describe below. Hence, our protocol

263 was to place the tethered honeybee in the centre of the arena, rest it comfortably on the

264 platform, and then commence the stimulus motion as soon as possible after platform

265 withdrawal (typically, within a second).

266

267 *Honeybees only exhibit flight behaviour during simulated forward motion*

268

269 Withdrawal of the platform always triggered wing beat activity. However, this activity

270 typically ceased seconds thereafter if there was no image motion (NIM). The abdomen would

271 then hang almost vertically and often curl inwards toward the head (Fig. 3). Similar

272 responses were observed when honeybees were exposed to backward image motion (BIM),

273 namely, image motion that simulated backward flight. In contrast, even on the very first test

274 flight, the majority of honeybees (76 out of 101) that experienced forward image motion

275 (FIM) – image motion that simulated forward flight -- exhibited continuous flight for the

276 entire duration of the visual stimulus. Presentation of FIM in the two front monitors and BIM

277 in the two rear monitors – or vice versa – also evoked no flight (unpublished observations).

278

279 *A novel 'streamlining' response observed during simulated forward image motion*

280

281 Bees presented with forward image motion responded not only with wing beat activity, but

282 also with a 'streamlining' response. As the speed of the image motion was increased, the

283 position of the abdomen would rise progressively and then remain in the elevated position for

284 the rest of the trial (see Fig. 3, and movie in Supplementary Material). The abdomen reached
285 its highest elevation (approximately -10°) at an image speed of 430 °/s and remained at this
286 elevation for all higher speeds, up to the maximum speed of 859 °/s. Thus, at speeds beyond
287 430 °/s, the streamlining response was maximal and approximately independent of stimulus
288 speed.

289

290 [Insert Fig. 3 here]

291

292 *Panoramic motion vision in honeybees*

293

294 Bees were also tested in the same arena with different combinations of only two active
295 monitors (the other two monitors were switched off, creating a black display). All tests were
296 conducted using the same stimulus protocol of ascending image speed. The bees exhibited a
297 streamlining response even with the two monitor setups. However, in this case they flew less
298 consistently, and for shorter periods. Fig. 4 shows the relationship between the response and
299 stimulus speed for various combinations of stimulation with two monitors: (i) left and right
300 front fields, (ii) left and right rear fields, (iii) left front and right rear fields, and (iv) right
301 front and left rear fields. Statistical analyses were performed to see whether the abdominal
302 responses for all of these four different two-monitor configurations differed significantly. The
303 two-way repeated measures ANOVA did not reveal any significant mains effect of monitor
304 configuration, $F(3, 18)=0.44$, $p=0.73$ (see Table A1).

305

306 However, it is clear that in comparison with the results obtained using four monitors the
307 responses obtained with two monitors are consistently lower. This is also reflected in the
308 statistical results. We find that there is a significant mains effect of monitor configuration,
309 $F(4, 24)=19.62$, $p<0.001$ (see Table A2), when the dataset includes responses from four and
310 all two-monitor configurations. Post-hoc pairwise comparison of the monitor configurations
311 at each OFR showed significant differences between the four-monitor configuration and each
312 two-monitor configuration , ($p<0.005$ with Bonferroni correction in all cases, see Table A2).

313

314 Furthermore, while the curve for four monitors is essentially flat for speeds greater than 430
315 °/s, the two-monitor curves exhibit a clear peak at stimulus speeds between 602-773 °/s (Fig.
316 4). With two monitors, similar response-versus-speed curves are obtained regardless of the
317 configuration of the monitors – all four configurations yield similar results (Fig. 4).

318

319   [Insert Fig. 4 here]

320

321   One should consider the possibility that the intermediate peak observed in the two-monitor

322   tuning curves arises as a result of fatigue during flight through the prolonged (72-second)

323   stimulus protocol, causing the response to diminish at the higher speeds. This is unlikely,

324   however, because the phenomenon is not observed with four-monitor stimulation.

325   Nevertheless, we performed control experiments with two monitors in which the stimulus

326   speed was not increased progressively, but instead held constant for the entire period of 72

327   seconds. Under these conditions, we found that the response was nearly constant throughout

328   the period of stimulation. This is shown in Fig. 5 for two different stimulus speeds. These

329   results demonstrate that the bell shaped speed tuning curves obtained with two-monitor

330   stimulation are not a consequence of response fatigue – they represent a variation of the

331   sensitivity of the response to the speed of the stimulus.

332

333   [Insert Fig. 5 here]

334

335   *Effect of stimulus contrast*

336   How sensitive is the streamlining response to variations in the contrast of the visual

337   environment? This was investigated by conducting experiments using the standard stimulus

338   protocol (as in the experiments of Figs 3 and 4) for different Michelson contrasts (C) of the

339   grating. The results are shown in Fig. 6. The profiles of the curves for C=0.72, C=0.54,

340   C=0.36 and C=0.29 are very similar in shape and height.

341

342   Statistical analyses were performed to examine whether the abdominal responses for all of

343   these four grating contrasts differed significantly. These analyses did not detect any

344   significant mains effect of contrast, $F(3, 15)=1.47$, $p=0.26$ (see Table A3). Consistent with

345   the ANOVA results, the corrected post-hoc pairwise comparisons between the non-zero

346   contrast conditions did not show any significant differences (in all cases, $p>0.75$). On the

347   other hand, when the abdominal responses obtained from the same bees for a grating contrast

348   of 0.0 were included for comparison, results showed that there was a significant mains effect

349   of contrast, $F(4, 20)=53.24$, $p<0.001$. Post-hoc pairwise comparison of contrast conditions at

350   each OFR showed significant differences between each zero contrast and all corresponding

351   non-zero contrast conditions (in all cases, $p<0.005$ with Bonferroni correction, see Table A4).

352

353   This means that the streamlining response goes from zero to a value that is close to its

354   maximum value when the contrast of the grating is increased from 0.0 to 0.29, and then

355   remains more or less constant for contrast values ranging from 0.29 to 0.72. In other words,

356   the streamlining response is relatively robust to changes in contrast in the mid-to high

357   contrast range of 0.29 – 0.72.

358

359   [Insert Fig. 6 here]

360

361   **Discussion**

362

363   Our results have revealed, for the first time, the existence of a visually-driven 'streamlining

364   response' in flying insects. This response, which can be elicited without exposing the insect

365   to any airflow, presumably serves to reduce the aerodynamic drag that would otherwise be

366   produced by the abdomen during real flight. While earlier studies with flying insects have

367   documented elevation of the abdomen during flight (Moth: Willmott and Ellington, 1997;

368   Bumblebee: Dudley and Ellington, 1990; *Drosophila*: David, 1978; Honeybee: Nachtigall et

369   al., 1971; Esch et al., 1975), they observed this elevation in free, un-tethered flight. Hence, it

370   is difficult to ascertain from these studies whether the raising of the abdomen was meditated

371   by the visual input, by mechanosensory signals driven by the wind, or simply by passive

372   mechanical raising of the abdomen by the wind. However, Zanker (1988) reports a cursory

373   observation of a small difference ($\pm 2°$) in abdominal deflection between backward image

374   motion and forward image motion in *Drosophila*. Our study demonstrates comprehensively

375   that the streamlining response can be elicited by a visual stimulus alone, namely, a moving

376   pattern, and documents its properties.

377

378   The streamlining response is highly selective to the direction of motion of the visual pattern.

379   Forward image motion (motion in the direction that would be experienced during forward

380   flight) creates a pronounced elevation of the abdomen. On the other hand, a stationary

381   pattern, or a pattern that moves in the opposite direction (simulating backward flight) does

382   not elicit any response – the abdomen remains in its lowered state (Fig. 3).

383

384   Panoramic stimulation with image motion seems to be critical for eliciting a strong

385   streamlining response. With four monitors, the response is significantly and substantially

12

stronger than that measured with two monitors, at all stimulus speeds (Fig. 4). The four-monitor stimulus produces a streamlining response that increases steadily with stimulus speed up to a speed of about 400 °/s, and then remains constant at this maximum value for all higher stimulus speeds. The two-monitor stimulus, on the other hand, yields a bell-shaped curve for response versus stimulus speed, exhibiting a peak at stimulus speeds in the range 602-773 °/s, regardless of the particular configuration of the two stimulating monitors (Fig. 4).

These findings reveal that, when studying visually evoked responses in flying insects, it is important to ensure that the stimulation covers all, or as much of the visual field of the insect as possible. Panoramic visual stimulation, which is what an insect would experience during actual flight in a real environment, reveals response properties that are very different from those produced by visual stimulation of restricted regions of the visual field. Consequently, many of the earlier studies of visually-evoked behaviour in insects that did not use panoramic, or nearly full-field stimulation, would have to be reassessed.

What causes four-monitor stimulation to be more effective than two-monitor stimulation? A simple possibility is that the responses of movement-detecting neurons that sample various sub-regions of the bee's panoramic visual environment are spatially summed to generate a command signal that drives the streamlining response. Stimulation of the visual system with four monitors, rather than two, would then produce a stronger streamlining response. This hypothesis of summation is also consistent with our observation that presentation of FIM in the two front monitors and BIM in the two rear monitors – or vice versa – also evokes no flight (data not shown), presumably because the oppositely-directed stimuli cancel each other out, in each case.

If such spatial summation does indeed occur, the summation must not be linear because the response-speed curve that is obtained with four monitors cannot be predicted accurately simply by scaling the two-monitor curve by a factor of two. However, the four-monitor curve can be explained if we postulate that the streamlining response is driven by a saturating summation of the responses of the various movement-detecting neurons. The possibility is supported by the observation that the standard deviations of the responses obtained with the four- monitor stimulus are consistently smaller than those obtained with two monitors, at

419   each of the tested speeds except for the lowest speed (172 °/s) – a property that is
420   characteristic of saturation at high response levels.

421

422   Can the saturation of the streamlining response be prevented by lowering the contrast of the
423   visual stimulus to reduce the strength of the movement signal? Evidently not. The data in Fig.
424   6 show that, with the four-monitor stimulation, the response curves obtained for grating
425   contrasts of 0.54, 0.36 and 0.29 are remarkably similar to, and not significantly different from
426   that obtained for a grating contrast of 0.72. This must mean that the responses of the
427   movement detecting neurons that drive the streamlining response are relatively insensitive to
428   variations of stimulus contrast in the range 0.29 – 0.72. This in turn implies that this
429   invariance to contrast must come about through an invariance of each movement-detecting
430   neuron's response to the stimulus, for contrasts exceeding about 0.3. The lamina neurons,
431   which are second-order neurons of the insect visual pathway, exhibit response saturation at
432   contrasts exceeding 0.4 (Laughlin, 1981). If these lamina neurons provide the inputs to the
433   movement–detecting neurons, their properties would partially account for the postulated
434   contrast invariance. Indeed, individual movement-detecting neurons in the insect visual
435   pathway show response invariance at contrasts exceeding about 0.3 (e.g. Dvorak et al., 1980).
436   Thus, all of the properties of the streamlining response that have been observed so far can be
437   explained by postulating phenomena occurring at two levels of the visual pathway: (a)
438   contrast invariance of the responses of the movement-detecting neurons and (b) saturating
439   summation of the responses of these movement-detecting neurons.

440

441   The finding that the streamlining response already attains a strength close to its maximum
442   value for sinusoidal gratings with a Michelson contrast as low as 0.29 - which corresponds to
443   a root-mean-square (RMS) contrast of 0.20 - is very compatible with the fact that natural
444   environments generally present RMS contrasts in the range of 0.2-0.3 (e.g. Frazor and
445   Geisler, 2006). Thus, the characteristics of the visually driven streamlining response are
446   tailored to the properties of the natural environment.

447

448   The study by Nacthigall and Hanauer-Thiesser (1992), measuring the aerodynamic drag that
449   is experienced by honeybees for various pitches of the abdomen, demonstrates clearly that
450   drag is reduced when the abdomen is raised, and is minimal when the abdomen is oriented
451   horizontally, i.e., parallel to the direction of flight, when it presents a minimal cross-section
452   to the horizontal airflow. Thus, the changes that we observe in abdominal pitch could indeed

453   reflect a visually driven response that serves to reduce drag as the perceived speed through
454   the environment is increased. Indeed, freely flying bees tend to hold the abdomen high when
455   cruising, and low when hovering or flying at slow speeds (Esch et al., 1975). In real flight,
456   however, bees should, at least in principle, be able to estimate their flight speed not just
457   through visual cues, but also through mechanosensory cues. For example, changes in
458   abdominal pitch could be mediated by a reflex that is driven by sensing airspeed as signaled
459   by the Johnston's organ at the base of the antennae, and/or other wind-sensitive hairs on the
460   head and body (Goodman, 2003). Additionally, the abdomen could simply be pushed up
461   passively at higher flight speeds by the increased aerodynamic pressure acting on the
462   underside of the abdomen and the legs (Nachtigall et al., 1971; Nachtigall and Hanauer-
463   Thiesser, 1992). Notwithstanding these other possibilities, our experiments, conducted with
464   tethered bees in still air, demonstrate clearly that vision plays an important role in tuning the
465   posture of the body during flight.
466   Nachtigall and Hanauer-Thiesser (1992) have shown experimentally, by blowing wind at
467   various velocities against the trunk of a honeybee, that the drag force increases as
468    $(velocity)^{1.5}$. This implies that when a bee increases its flight speed from a value that is close
469   to hover (say, 5 cm/sec) to a value that is typical of cruise (say, 10 m/sec) the drag would
470   increase by a factor of about 2,800, if the body did not change its posture or shape. The same
471   study finds that decreasing the angle of attack of the body from 20° to 0° can reduce the drag
472   by about 50%, which would lead to a significant increase of flight speed and/or a significant
473   saving of energy over a long flight. Thus, it would appear that actively raising the abdomen
474   indeed produces a significant and beneficial streamlining effect.
475   Finally, the variation of posture with flight speed may represent more than just a streamlining
476   response- it may reflect the fundamental means by which the insect adjusts its thrust and lift
477   to achieve flight at various speeds. Horizontal flight at higher speeds requires the wings to
478   produce not only increased thrust, but also decreased lift – because the abdomen and the legs
479   generate greater passive aerodynamic lift at higher speeds (Nachtigall and Hanauer-Thiesser,
480   1992). It has been suggested that, like the fruitfly *Drosophila* (Götz and Wandell, 1984;
481   Zanker, 1988; Vogel, 1996), honeybees are unable to vary the direction of the net force
482   vector that is generated by their wings, relative to their body axis (Nachtigall et al., 1971;
483   Esch et al., 1975; Taylor, 2001). If this is indeed the case, then the only way to increase flight
484   speed - and to continue to fly horizontally - would be to decrease the angle of elevation of the
485   force vector by pitching the thorax downwards, and raising the abdomen (Nachtigall et al.,

486   1971). Thus, our observed changes in abdominal pitch may reflect a part of this underlying

487   strategy of flight control. However, exactly how changes in abdominal elevation can affect

488   changes in the pitch of the thorax is not fully understood, although a model examining these

489   changes has been proposed for the fruitfly *Drosophila (*Zanker, 1988), and the answer would

490   depend partly on the (as yet undetermined) location of the insect's centre of gravity relative

491   to the point of action of the net force vector generated by the wings (Taylor, 2001).

492

493   It should be noted that the responses described in the present study have been obtained using

494   an 'open loop' mode of experimentation in which the insect is responding to the stimulus that

495   it receives, but is unable to influence the stimulus. Our experiments reveal that body posture

496   is strongly influenced by the visual stimulus, but they do not tell us whether an unrestrained

497   bee in free flight controls its flight speed (and therefore the image speed that it experiences)

498   by adjusting its body posture. Further studies, conducted using a 'closed loop' paradigm in

499   which the tethered insect is able to freely adjust the pitch of its body, and where the measured

500   thrust and lift are used to control the motion of the visual panorama as well as the airflow

501   appropriately, should provide a more complete understanding of the phenomenon that we

502   have uncovered here.

503

504

505

506

507 **List of symbols and abbreviations**

508

509 OFR – optic flow rate

510 NIM – no image motion

511 BIM – backward image motion

512 FIM – forward image motion

513 C – contrast

514 I_{min} – minimum intensity

515 I_{max} – maximum intensity

516 RMS – root-mean-square

517

518 **Appendix**

519

520 Table A1. Statistical results for comparisons made between the various two-monitor

521 configurations.

522 Table A2. Statistical results for comparisons made between the two- and four-monitor

523 configurations.

524 Table A3. Statistical results for comparisons made between the four non-zero contrast

525 conditions.

526 Table A4. Statistical results for comparisons made between control (zero) and the four

527 contrast conditions.

528

529

530

531

532

533

534 **Acknowledgements**

539

540   **References**

542   **Bailey, J.** (1997). *How fish swim*. New York: Benchmark Books.

543   **Baird, E., Srinivasan, M. V., Zhang, S. and Cowling, A.** (2005). Visual control of flight
544   speed in honeybees. *J. Exp. Biol.* **208**, 3895-3905.

545   **Batchelor, G. K.** (2000). *An introduction to fluid dynamics*. Cambridge Mathematical
546   Library (2nd ed.): Cambridge University Press.

547   **Chadwick, L. E**. (1953). The flight muscles and their control. In *Insect Physiology* (ed. K. D.
548   Roeder), pp. 648-655. New York: Wiley.

549   **Chittka, L., Vorobyev, M., Shmida, A., and Menzel, R.** (1993). Bee colour vision- the
550   optimal system for the discrimination of flower colours with three spectral photoreceptor
551   types? In: *Sensory Systems of Arthropods* (ed. K. Weise, F. G. Gribakin, A. G. Popov and G.
552   Renninger), pp. 211–218. Basel: Birkhauser Verlag.

553   **Collett. T., Nalbach, H-O., and Wagner, H**. (1993). Visual stabilization in arthropods. In
554   *Visual Motion and its Role in the Stabilization of Gaze* (ed F. Miles and J. Wallman), pp.
555   239-263. Amsterdam: Elsevier.

556   **David, C. T**. (1978). The relationship between body angle and flight speed in free-flying
557   *Drosophila. Physiol. Entomol.* **3***, 191-195.

558   **David, C. T.** (1979). Optomotor control of speed and height by free-flying *Drosophila*. *J.
559   Exp. Biol.* **82**, 389-392.

560   **David, C. T.** (1982). Compensation for height in the control of groundspeed by *Drosophila*
561   in a new 'barber's pole' wind tunnel. *J. Comp. Physiol. A*. **147**, 485-493.

562   **Dvorak, D., Srinivasan, M. V. and French, A. S.** (1980). The contrast sensitivity of fly
563   movement-detecting neurons. *Vision Res*. **20**, 397-407.

564   **Dudley, R. and Ellington, C. P.** (1990). Mechanics of forward flight in bumblebees. I.
565   Kinematics and morphology. *J. Exp. Biol*. **148**, 19-52.

566   **Egelhaaf, M., Grewe, J., Karmeier, K., Kern, R., Kurtz, R., and Warzecha, A.** (2004).
567   Novel approaches to visual information processing in insects: Case studies on neuronal
568   computations in the blowfly. In *Methods in Insect Sensory Neuroscience* (ed T. A.
569   Christensen) pp. 185-212. Boca Raton, London, New York: CRC Press.

570   **Esch, H., Nachtigall, W. and Kogge S. N.** (1975). Correlations between aerodynamic
571   output, electrical activity in the indirect flight muscles and wing positions of bees flying in a
572   servomechanically controlled wind tunnel. *J. Comp. Physiol.* **100**, 147-159.

573   **Fraenkel, G.** (1932). Untersuchungen über die Koordination von Reflexen und automatisch-

574   nervösen Rhythmen bei Insekten. I. Die Flugreflexe der Insekten und ihre Koordination.

575   *Zeitschr. vergleich. Physiol.* **16**, 371-393.

576   **Fry, S. N., Rohrseitz, N., Straw, A. D. and Dickinson, M. H**. (2009). Visual flight speed

577   control in *Drosophila melanogaster*. *J. Exp. Biol*. **212**, 1120-1130.

578   **Frazor, R. A. and Geisler, W. S.** (2006). Local luminance and contrast in natural images.

579   *Vision Res*. **46**, 1585-1598.

580   **Goodman, L.** (2003). *Form and Function in the Honeybee*. Cardiff, U.K: International Bee

581   Research Association.

582   **Götz, K. G**. (1965). Die optischen Übertragungseigenschaften der Komplexaugen von

583   *Drosophila*. *Kybernetik.* **2**, 215–21.

584   **Götz, K. G. and Wandel, U.** (1984). Optomotor control of the force of flight in *Drosophila*

585   and *Musca*.II. Covariance of lift and thrust in still air. *Biol. Cybern*. **51**, 135-139.

586   **Krapp, H. G. and Hengstenberg, R.** (1996). Estimation of self-motion by optic flow

587   processing in single visual interneurons. *Nature* **384**, 463-466.

588   **Laughlin, S. B.** (1981). A simple coding procedure enhances a neuron's information

589   capacity. *Z. Naturforsch.* **36c**, 910-912.

590   **Menzel, R. and Blakers, M.** (1976). Color receptors in the bee eye - morphology and

591   spectral sensitivity. *J. Comp. Physiol.* **108**, 1 l-33.

592   **Michelson, A. A.** (1927). *Studies in Optics*. Chicago: The University of Chicago Press.

593   **Nachtigall, W. and Hanauer-Thieser, U.** (1992). Flight of the honeybee.V. Drag and lift

594   coefficients of the bee's body; implications for flight dynamics. *J. Comp. Physiol., B* **162**,

595   267-277.

596   **Nachtigall, W., Widmann, R. and Renner, M.** (1971). Uber den "ortsfesten" freien Flug

597   von Bienen in einem Saugkanal. *Apidologie* **2**, 271-282.

598   **Reichardt, W.** (1969). *Processing of optical data by organisms and by machines*. New York:

599   Academic Press.

600   **Schmidt-Nielsen, K.** (1984). *Scaling: why is animal size so important?* Cambridge and New

601   York: Cambridge University Press.

602   **Srinivasan, M. V. and Bernard, G. D.** (1977). The pursuit response of the housefly and its

603   interaction with the optomotor response. *J. Comp. Physiol., A* **115**, 101–117.

604   **Srinivasan, M. V., Lehrer, M., Kirchner, W. and Zhang, S. W.** (1991). Range perception

605   through apparent image speed in freely flying honeybees. *Vis. Neurosci.* **6**, 519–535.

606   **Srinivasan, M. V. and Zhang, S. W.** (1997). Visual control of honeybee flight. In
607   *Orientation and Communication in Arthropods* (ed. M. Lehrer), pp. 95-114. Basel, Boston,
608   Berlin: Birkhauser Verlag.

609   **Srinivasan, M. V., Zhang, S. W., Chahl, J. S., Barth, E. and Venkatesh, S.** (2000). How
610   honeybees make grazing landings on flat surfaces. *Biol. Cybern*. **83**, 171-183.

611   **Srinivasan, M. V., Zhang, S. W. and Chandrashekara, K.** (1993). Evidence for two
612   distinct movement-detecting mechanisms in insect vision. *Naturwissenschaften* **80**, 38–41.

613   **Srinivasan, M. V., Zhang, S. W., Lehrer, M. and Collett, T.** (1996). Honeybee navigation
614   *en route* to the goal: visual flight control and odometry. *J. Exp. Biol.* **199**, 237-244.

615   **Tammero, L. F. and Dickinson, M. H.** (2002). Collision-avoidance and landing responses
616   are mediated by separate pathways in the fruit fly, *Drosophila melanogaster*. *J. Exp. Biol.*
617   **205**, 2785-2798.

618   **Taylor, G. K.** (2001). Mechanics and aerodynamics of insect flight control. *Biol. Rev*. **76**,
619   449-471.

620   **Willmott, A. P. and Ellington, C. P.** (1997). The mechanics of flight in the hawkmoth
621   *Manduca Sexta*. I. Kinematics of hovering and forward flight. *J. Exp. Biol*. **200**, 19-52.

622   **Vogel, S.** (1966). Flight in Drosophila. I. Flight performance of tethered flies. *J. Exp. Biol*.
623   **44**, 567-578.

624   **Zanker, J. M.** (1988). On the mechanism of speed and altitude control in *Drosophila*
625   *melanogaster. Physiol. Entomol.* **13**, 351-361.

626

627

Figure legends

629

630 **Figure 1.** The physical and virtual reality setup for tethered bee experiments. (A) Honeybees

631 were tethered to the horizontal end of an L-shaped metallic rod. Flight was initiated by

632 lowering a supporting platform. (B) Each honeybee was placed in the centre of the arena

633 composed of four monitors. A video camera was used to film a side view of the bee in flight.

634 (C) The virtual scene consisted of an infinite tunnel composed two walls lined with vertically

635 oriented red and white sinusoidal gratings. The honeybee was at a virtual distance of X units

636 from each of the tunnel walls, and experienced virtual forward motion at a speed of Y units

637 per display frame.

638

639 **Figure 2.** Illustration of the measurement of the streamlining response, defined as the

640 orientation of the abdomen relative to the thorax. The upper row of sketches illustration the

641 definition of the response, and the lower row show two examples of how this is used to

642 measure the response. Details in text.

643

644 **Figure 3.** Comparison of streamlining responses induced by forward image motion (FIM),

645 no image motion (NIM) and backward image motion (BIM). The grey staircase displays the

646 progressively ascending stimulus speed (see Methods). Each data point shows mean abdomen

647 angle ± s.e.m. Note the comparatively small variability in the responses when bees were

648 experiencing forward image motion.

649

650 **Figure 4.** Streamlining responses of tethered bees in experiments using various

651 configurations of two monitors (colored symbols), compared with the four-monitor

652 configuration (black symbols). All flights were presented with the ascending image motion

653 speed protocol, as indicated by the grey staircase. Each data point shows mean abdomen

654 angle ± s.d. Data comprised only from bees that experienced all 5 monitor configurations

655 (n=7).

656

657 **Figure 5.** Control experiments showing the variation of the streamlining response with time

658 in a protocol in which the stimulus speed was held constant throughout the experiment at 355

659 °/s or at 526 °/sec. There is no systematic variation of the mean response with time,

660 indicating that response fatigue is not a factor influencing the results in the experiments of

661 figure 4. Each data point shows the mean abdomen angle ± s.e.m.

662

663   **Figure 6.** Effect of stimulus contrast on the streamlining response. Variation of abdomen

664   orientation with stimulus speed for five different contrasts, as shown in the index. Each data

665   point shows the mean abdomen angle ± s.e.m. (n=6).

A.

B. Physical world

camera

C. Virtual world

Image
motion

Y speed

X
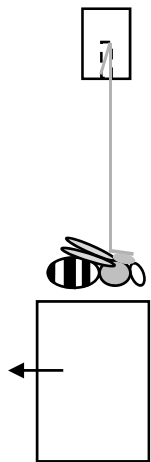
Figure 1
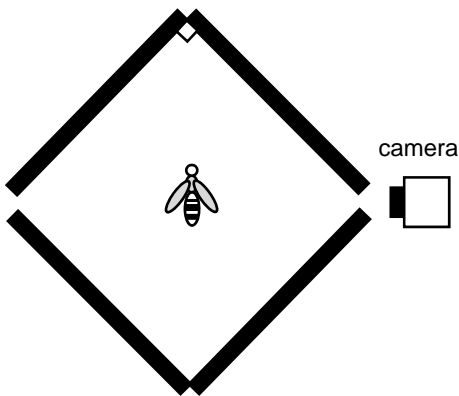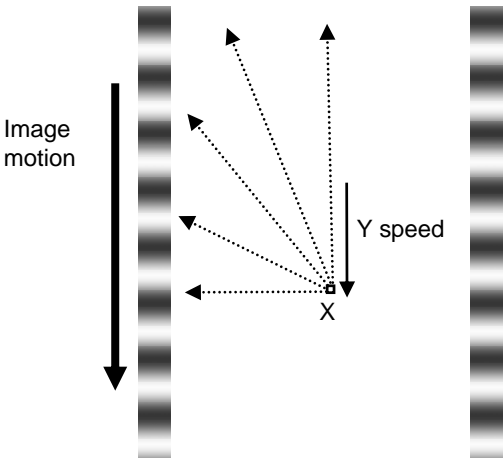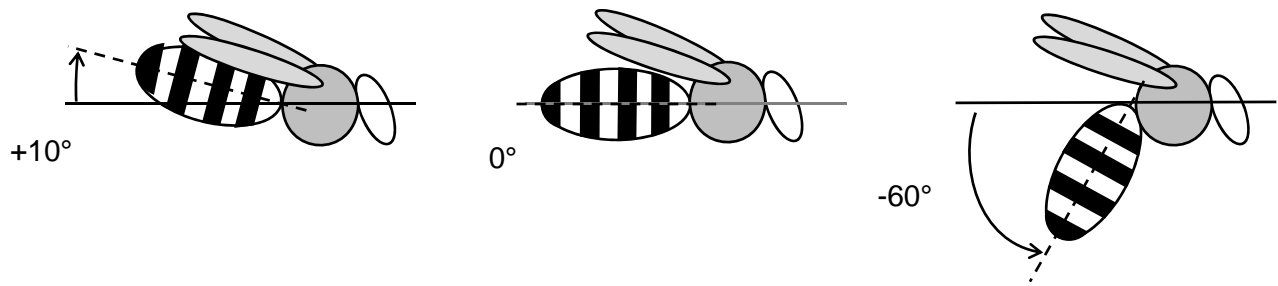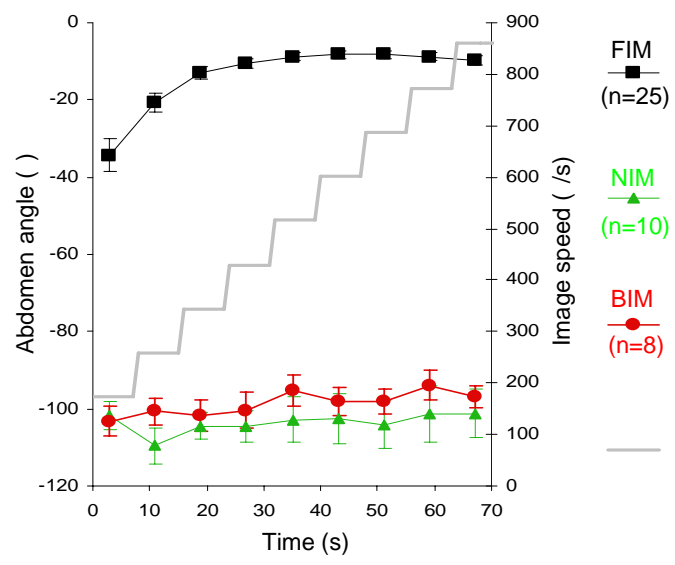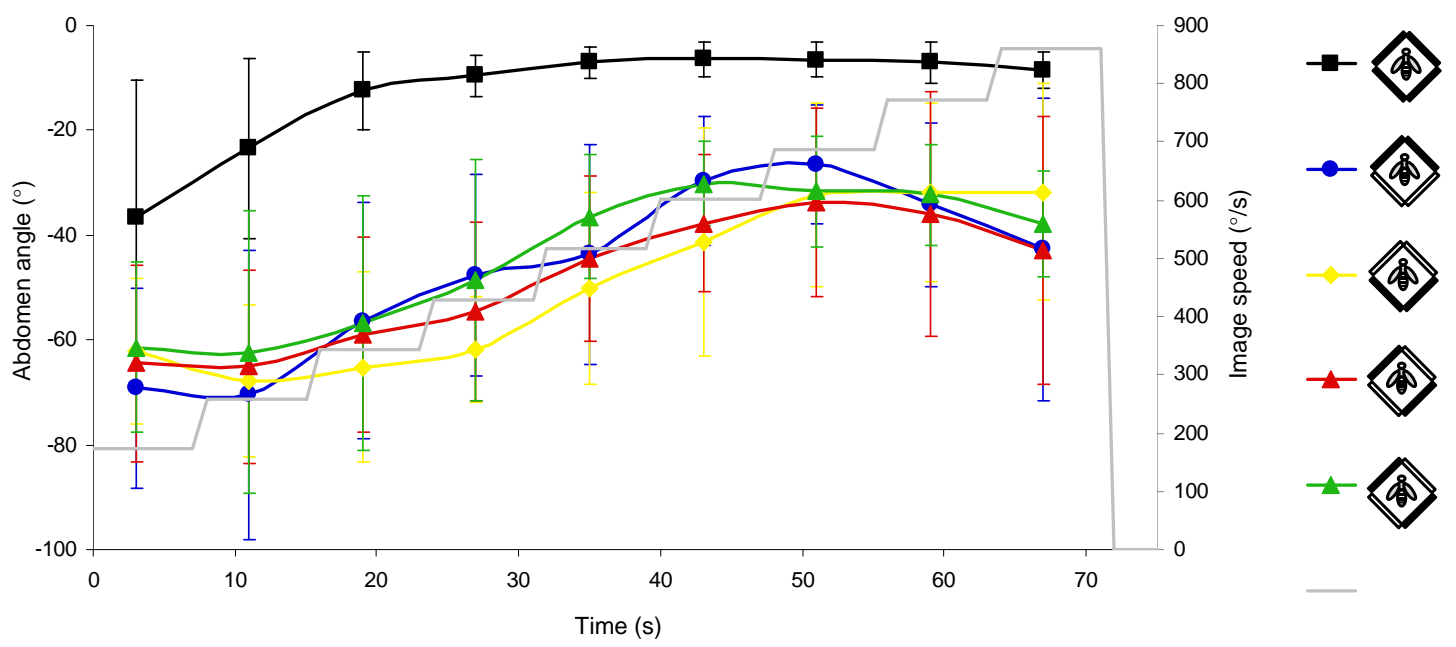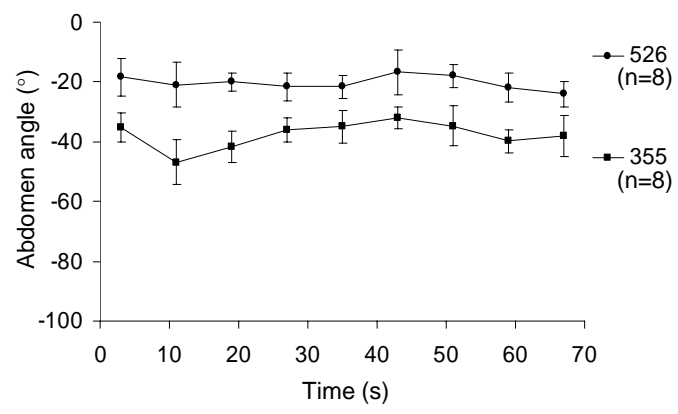
Figure 2

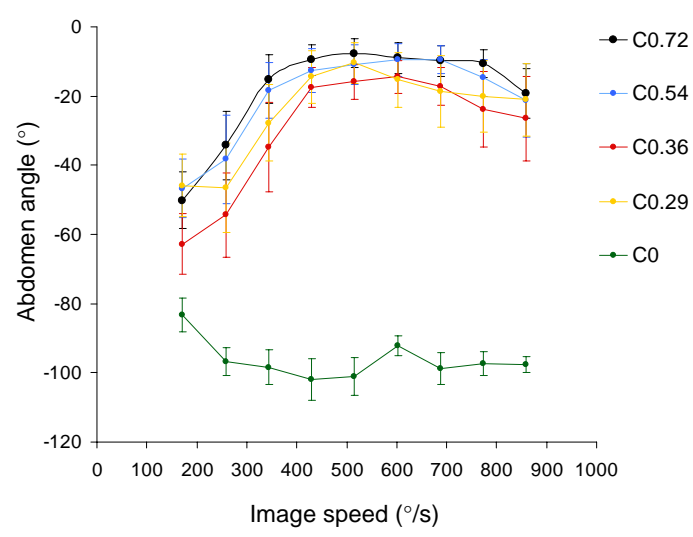Figure 3

Figure 4

Figure 5

Figure 6

Appendix

Table A1. Statistical results for comparisons made between the various two-monitor configurations.

Mauchly's Test of Sphericity[b]

Within Subjects Effect	Mauchly's W	Approx. Chi-Square	df	Sig.	Epsilon[a]		
					Greenhouse-Geisser	Huynh-Feldt	Lower-bound
MonConfig	.195	7.713	5	.181	.585	.808	.333
OFR	.000	.	35	.	.193	.246	.125
MonConfig * OFR	.000	.	299	.	.155	.437	.042

Tests the null hypothesis that the error covariance matrix of the orthonormalized transformed dependent variables is proportional to an identity matrix.

a. May be used to adjust the degrees of freedom for the averaged tests of significance. Corrected tests are displayed in the Tests of Within-Subjects Effects table.

b. Design: Intercept

Within Subjects Design: MonConfig + OFR + MonConfig * OFR

Tests of Within-Subjects Effects

Source		Type III Sum of Squares	df	Mean Square	F	Sig.
MonConfig	Sphericity Assumed	1029.372	3	343.124	.437	.729
	Greenhouse-Geisser	1029.372	1.756	586.308	.437	.632
	Huynh-Feldt	1029.372	2.424	424.593	.437	.691
	Lower-bound	1029.372	1.000	1029.372	.437	.533
Error(MonConfig)	Sphericity Assumed	14138.202	18	785.456		
	Greenhouse-Geisser	14138.202	10.534	1342.135		
	Huynh-Feldt	14138.202	14.546	971.949		
	Lower-bound	14138.202	6.000	2356.367		
OFR	Sphericity Assumed	42785.115	8	5348.139	12.910	.000
	Greenhouse-Geisser	42785.115	1.541	27768.953	12.910	.003
	Huynh-Feldt	42785.115	1.970	21716.948	12.910	.001
	Lower-bound	42785.115	1.000	42785.115	12.910	.011
Error(OFR)	Sphericity Assumed	19885.242	48	414.276		
	Greenhouse-Geisser	19885.242	9.245	2151.030		
	Huynh-Feldt	19885.242	11.821	1682.231		
	Lower-bound	19885.242	6.000	3314.207		
MonConfig * OFR	Sphericity Assumed	2954.672	24	123.111	.811	.718
	Greenhouse-Geisser	2954.672	3.714	795.521	.811	.524
	Huynh-Feldt	2954.672	10.499	281.428	.811	.624

	Lower-bound	2954.672	1.000	2954.672	.811	.402
Error(MonConfig*OFR)	Sphericity Assumed	21856.786	144	151.783		
	Greenhouse-Geisser	21856.786	22.285	980.793		
	Huynh-Feldt	21856.786	62.993	346.971		
	Lower-bound	21856.786	6.000	3642.798		

Table A2. Statistical results for comparisons made between the two- and four-monitor configurations.

Mauchly's Test of Sphericity[b]

	Mauchly's W	Approx. Chi-Square	df	Sig.	Epsilon[a]		
					Greenhouse-Geisser	Huynh-Feldt	Lower-bound
MonConfig	.173	7.739	9	.589	.625	1.000	.250
OFR	.000	.	35	.	.182	.226	.125
MonConfig * OFR	.000	.	527	.	.128	.439	.031

Tests the null hypothesis that the error covariance matrix of the orthonormalized transformed dependent variables is proportional to an identity matrix.

a. May be used to adjust the degrees of freedom for the averaged tests of significance. Corrected tests are displayed in the Tests of Within-Subjects Effects table.

b. Design: Intercept

Within Subjects Design: MonConfig + OFR + MonConfig * OFR

Tests of Within-Subjects Effects

Source		Type III Sum of Squares	df	Mean Square	F	Sig.
MonConfig	Sphericity Assumed	59954.038	4	14988.509	19.617	.000
	Greenhouse-Geisser	59954.038	2.501	23968.601	19.617	.000
	Huynh-Feldt	59954.038	4.000	14988.509	19.617	.000
	Lower-bound	59954.038	1.000	59954.038	19.617	.004
Error(MonConfig)	Sphericity Assumed	18336.969	24	764.040		
	Greenhouse-Geisser	18336.969	15.008	1221.801		
	Huynh-Feldt	18336.969	24.000	764.040		
	Lower-bound	18336.969	6.000	3056.162		
OFR	Sphericity Assumed	45500.309	8	5687.539	14.298	.000
	Greenhouse-Geisser	45500.309	1.457	31227.072	14.298	.003
	Huynh-Feldt	45500.309	1.805	25209.218	14.298	.001
	Lower-bound	45500.309	1.000	45500.309	14.298	.009
Error(OFR)	Sphericity Assumed	19093.636	48	397.784		

	Greenhouse-Geisser	19093.636	8.742	2184.008		
	Huynh-Feldt	19093.636	10.829	1763.122		
	Lower-bound	19093.636	6.000	3182.273		
MonConfig * OFR	Sphericity Assumed	6165.922	32	192.685	1.379	.098
	Greenhouse-Geisser	6165.922	4.100	1503.859	1.379	.270
	Huynh-Feldt	6165.922	14.053	438.751	1.379	.182
	Lower-bound	6165.922	1.000	6165.922	1.379	.285
Error(MonConfig*OFR)	Sphericity Assumed	26836.069	192	139.771		
	Greenhouse-Geisser	26836.069	24.600	1090.880		
	Huynh-Feldt	26836.069	84.320	318.264		
	Lower-bound	26836.069	6.000	4472.678		

Pairwise Comparisons

(I) MonConfig	(J) MonConfig	Mean Difference (I-J)	Std. Error	Sig.[a]	95% Confidence Interval for Difference[a]	
					Lower Bound	Upper Bound
1	2	2.648	6.919	1.000	-27.218	32.515
	3	-2.548	2.243	1.000	-12.228	7.133
	4	1.979	4.276	1.000	-16.478	20.436
	5	-33.673*	4.424	.003	-52.771	-14.575
2	1	-2.648	6.919	1.000	-32.515	27.218
	3	-5.196	5.617	1.000	-29.442	19.050
	4	-.670	5.595	1.000	-24.821	23.482
	5	-36.321*	5.559	.006	-60.317	-12.326
3	1	2.548	2.243	1.000	-7.133	12.228
	2	5.196	5.617	1.000	-19.050	29.442
	4	4.526	3.948	1.000	-12.515	21.568
	5	-31.125*	3.936	.002	-48.117	-14.133
4	1	-1.979	4.276	1.000	-20.436	16.478
	2	.670	5.595	1.000	-23.482	24.821
	3	-4.526	3.948	1.000	-21.568	12.515
	5	-35.652*	5.194	.005	-58.073	-13.230
5	1	33.673*	4.424	.003	14.575	52.771
	2	36.321*	5.559	.006	12.326	60.317
	3	31.125*	3.936	.002	14.133	48.117
	4	35.652*	5.194	.005	13.230	58.073

Based on estimated marginal means

a. Adjustment for multiple comparisons: Bonferroni.

*. The mean difference is significant at the .05 level.

Table A3. Statistical results for comparisons made between the four non-zero contrast conditions.

Mauchly's Test of Sphericity[b]

	Mauchly's W	Approx. Chi-Square	df	Sig.	Epsilon[a]		
					Greenhouse-Geisser	Huynh-Feldt	Lower-bound
Contrast	.608	1.853	5	.873	.745	1.000	.333
OFR	.000	.	35	.	.275	.499	.125
Contrast * OFR	.000	.	299	.	.104	.214	.042

Tests the null hypothesis that the error covariance matrix of the orthonormalized transformed dependent variables is proportional to an identity matrix.

a. May be used to adjust the degrees of freedom for the averaged tests of significance. Corrected tests are displayed in the Tests of Within-Subjects Effects table.

b. Design: Intercept

Within Subjects Design: MonConfig + OFR + MonConfig * OFR

Tests of Within-Subjects Effects

Source		Type III Sum of Squares	df	Mean Square	F	Sig.
Contrast	Sphericity Assumed	4084.904	3	1361.635	1.467	.263
	Greenhouse-Geisser	4084.904	2.234	1828.600	1.467	.274
	Huynh-Feldt	4084.904	3.000	1361.635	1.467	.263
	Lower-bound	4084.904	1.000	4084.904	1.467	.280
Error(Contrast)	Sphericity Assumed	13921.102	15	928.073		
	Greenhouse-Geisser	13921.102	11.169	1246.351		
	Huynh-Feldt	13921.102	15.000	928.073		
	Lower-bound	13921.102	5.000	2784.220		
OFR	Sphericity Assumed	40476.934	8	5059.617	13.218	.000
	Greenhouse-Geisser	40476.934	2.197	18423.584	13.218	.001
	Huynh-Feldt	40476.934	3.989	10146.225	13.218	.000
	Lower-bound	40476.934	1.000	40476.934	13.218	.015
Error(OFR)	Sphericity Assumed	15310.864	40	382.772		
	Greenhouse-Geisser	15310.864	10.985	1393.786		
	Huynh-Feldt	15310.864	19.947	767.585		
	Lower-bound	15310.864	5.000	3062.173		
Contrast * OFR	Sphericity Assumed	1688.328	24	70.347	.599	.927
	Greenhouse-Geisser	1688.328	2.486	679.146	.599	.599
	Huynh-Feldt	1688.328	5.137	328.632	.599	.705
	Lower-bound	1688.328	1.000	1688.328	.599	.474

Error(Contrast*OFR)	Sphericity Assumed	14097.780	120	117.482		
	Greenhouse-Geisser	14097.780	12.430	1134.193		
	Huynh-Feldt	14097.780	25.687	548.825		
	Lower-bound	14097.780	5.000	2819.556		

Table A4. Statistical results for comparisons made between control (zero) and four contrast conditions.

Mauchly's Test of Sphericity[b]

| | Mauchly's W | Approx. Chi-Square | df | Sig. | Epsilon[a] | | |
					Greenhouse-Geisser	Huynh-Feldt	Lower-bound
Contrast	.266	4.527	9	.891	.684	1.000	.250
OFR	.000	.	35	.	.294	.572	.125
Contrast * OFR	.000	.	527	.	.077	.156	.031

Tests the null hypothesis that the error covariance matrix of the orthonormalized transformed dependent variables is proportional to an identity matrix.

a. May be used to adjust the degrees of freedom for the averaged tests of significance. Corrected tests are displayed in the Tests of Within-Subjects Effects table.

b. Design: Intercept

Within Subjects Design: MonConfig + OFR + MonConfig * OFR

Tests of Within-Subjects Effects

Source		Type III Sum of Squares	df	Mean Square	F	Sig.
Contrast	Sphericity Assumed	235379.647	4	58844.912	53.239	.000
	Greenhouse-Geisser	235379.647	2.737	85991.499	53.239	.000
	Huynh-Feldt	235379.647	4.000	58844.912	53.239	.000
	Lower-bound	235379.647	1.000	235379.647	53.239	.001
Error(Contrast)	Sphericity Assumed	22105.838	20	1105.292		
	Greenhouse-Geisser	22105.838	13.686	1615.190		
	Huynh-Feldt	22105.838	20.000	1105.292		
	Lower-bound	22105.838	5.000	4421.168		
OFR	Sphericity Assumed	28356.376	8	3544.547	10.672	.000
	Greenhouse-Geisser	28356.376	2.352	12053.893	10.672	.002
	Huynh-Feldt	28356.376	4.576	6196.923	10.672	.000
	Lower-bound	28356.376	1.000	28356.376	10.672	.022
Error(OFR)	Sphericity Assumed	13285.319	40	332.133		
	Greenhouse-Geisser	13285.319	11.762	1129.480		
	Huynh-Feldt	13285.319	22.879	580.667		

	Lower-bound	13285.319	5.000	2657.064		
Contrast * OFR	Sphericity Assumed	15339.390	32	479.356	4.126	.000
	Greenhouse-Geisser	15339.390	2.450	6261.070	4.126	.037
	Huynh-Feldt	15339.390	4.980	3080.054	4.126	.007
	Lower-bound	15339.390	1.000	15339.390	4.126	.098
Error(Contrast*OFR)	Sphericity Assumed	18590.789	160	116.192		
	Greenhouse-Geisser	18590.789	12.250	1517.638		
	Huynh-Feldt	18590.789	24.901	746.583		
	Lower-bound	18590.789	5.000	3718.158		

Pairwise Comparisons

(I) Contrast	(J) Contrast	Mean Difference (I-J)	Std. Error	Sig.[a]	95% Confidence Interval for Difference[a]	
					Lower Bound	Upper Bound
1 (C=0)	2	-71.907[*]	8.769	.004	-113.766	-30.048
	3	-66.671[*]	6.882	.002	-99.519	-33.822
	4	-76.146[*]	6.158	.001	-105.540	-46.752
	5	-77.961[*]	6.399	.001	-108.507	-47.415
2 (C=0.29)	1	71.907[*]	8.769	.004	30.048	113.766
	3	5.237	7.055	1.000	-28.441	38.915
	4	-4.239	4.111	1.000	-23.862	15.384
	5	-6.054	6.348	1.000	-36.356	24.249
3 (C=0.36)	1	66.671[*]	6.882	.002	33.822	99.519
	2	-5.237	7.055	1.000	-38.915	28.441
	4	-9.475	6.308	1.000	-39.585	20.634
	5	-11.290	5.040	.752	-35.349	12.769
4 (C=0.54)	1	76.146[*]	6.158	.001	46.752	105.540
	2	4.239	4.111	1.000	-15.384	23.862
	3	9.475	6.308	1.000	-20.634	39.585
	5	-1.815	5.837	1.000	-29.675	26.045
5 (C=0.72)	1	77.961[*]	6.399	.001	47.415	108.507
	2	6.054	6.348	1.000	-24.249	36.356
	3	11.290	5.040	.752	-12.769	35.349
	4	1.815	5.837	1.000	-26.045	29.675

Based on estimated marginal means

a. Adjustment for multiple comparisons: Bonferroni.

*. The mean difference is significant at the .05 level.